

Spatiotemporal model-based index development for Bering Sea and Aleutian Islands crab stocks

Update for Crab Plan Team modeling workshop

Caitlin Stern^{1,2}, Emily Ryznar^{3,4}, and Jon Richar^{3,5}

¹ Alaska Department of Fish and Game

²caitlin.stern@alaska.gov

³NOAA Fisheries

⁴emily.ryznar@noaa.gov

⁵jon.richar@noaa.gov

January 2025

Introduction

The goal of this investigation was to develop spatiotemporal model-based indices of abundance for three Bering Sea and Aleutian Islands (BSAI) crab stocks: Tanner crab (*Chionoecetes bairdi*), Norton Sound red king crab (*Paralithodes camtschaticus*), and St. Matthew Island blue king crab (*Paralithodes platypus*). Research suggests that spatiotemporal model-based indices can be more robust to survey changes than are design-based indices, though the models must be well-specified (Yalcin et al. 2023). Spatiotemporal model-based indices are used in North Pacific Fishery Management Council (NPFMC) groundfish stock assessments for species including Eastern Bering Sea (EBS) walleye pollock (*Gadus chalcogrammus*) and EBS Pacific cod (*Gadus macrocephalus*), both of which use the vector-autoregressive spatial temporal (VAST) approach (Thorson 2019) to produce indices used in the assessments (Ianelli et al. 2024; Barbeaux et al. 2024). Previous BSAI crab stock assessments have presented models using spatiotemporal model-based indices (e.g., Ianelli et al. 2017), although these models were not accepted for harvest specifications (SSC 2017).

We generated biomass and abundance estimates using the R package *sdmTMB* (Anderson et al. 2022), which uses geostatistical time series data to estimate spatial and spatiotemporal generalized linear mixed effects models. This approach allows for index standardization when the set of stations surveyed is not consistent across years: one can generate a spatial grid that covers the area of interest, predict from the model onto that grid, and sum the predicted biomass to obtain an area-weighted biomass index that is independent of sampling locations (Anderson et al. 2022).

All three stock assessments for the crab stocks presented here use data from the National Marine Fisheries Service (NMFS) EBS bottom trawl survey (Stockhausen 2024; Hamazaki 2024; Stern and Palof 2024). The St. Matthew Island blue king crab stock assessment also uses data from the Alaska Department of Fish and Game (ADF&G) St. Matthew Island blue king crab pot survey, while the Norton Sound red king crab stock assessment uses data from the NMFS Northern Bering Sea bottom trawl survey and the ADF&G Norton Sound red king crab trawl survey.

Spatiotemporal model-based index development is expected to confer distinct advantages for each of the three stocks. For the St. Matthew Island blue king crab stock, standardizing the survey indices could allow the assessment to use the existing survey data more rigorously. The NMFS EBS trawl survey is undergoing changes including dropping the high sampling density “corner stations” near St. Matthew Island from 2024 onward (DePhilippo et al. 2023; Stern & Palof 2024); index standardization will allow the assessment to continue using the full time series of data despite changes in the spatial footprint of the survey. For Norton

Sound red king crab, a model-based approach could provide a more consistent way to combine the three existing trawl survey data sets into a single index of abundance.

Methods

We fit models using the R package *sdmTMB*.

A number of decision points arise when fitting models using *sdmTMB*, including:

- The resolution of the spatial mesh used in fitting the model. A higher number of knots, specified when creating the spatial mesh using the `make_mesh()` function, indicates a higher resolution mesh. Few guidelines exist to aid in selection of an appropriate mesh resolution for a given dataset.
- The spatiotemporal random fields estimation method. The spatiotemporal random fields can be estimated as independent and identically distributed (IID), first-order autoregressive (AR1), a random walk, or fixed at zero.
- The model family. Many options exist, including `tweedie()`, `delta_gamma()`, and `delta_lognormal()`.

For each stock, we present a range of models to show the effects of choices at each of these decision points. After fitting models, we used the following steps for model evaluation:

- Run the `sdmTMB::sanity()` function. Output of this function for a model that passes all sanity checks looks like this:
 - Non-linear minimizer suggests successful convergence
 - Hessian matrix is positive definite
 - No extreme or very small eigenvalues detected
 - No gradients with respect to fixed effects are ≥ 0.001
 - No fixed-effect standard errors are NA
 - No standard errors look unreasonably large
 - No sigma parameters are < 0.01
 - No sigma parameters are > 100
 - Range parameter doesn't look unreasonably large
- If a model passed all the sanity checks, we used the R package *DHARMa* (Hartig 2022) to calculate the DHARMa residuals using the function `DHARMa::dharma_residuals()`. Models that did not pass the sanity checks were excluded from further consideration.
- We tested for quantile deviations, under/overdispersion, outliers, and zero inflation using the functions `DHARMa::testQuantiles()`, `DHARMa::testDispersion()`, `DHARMa::testOutliers()`, and `DHARMa::testZeroInflation()`, respectively.
- We evaluated model predictive log-likelihood (the predictive ability of the model for new observations; Anderson *et al.* 2024) using the function `sdmTMB_cv()`. This function measures model predictive log-likelihood by holding out subsets of the data in turn and using each as a test set. These subsets of data are termed “folds” and the number of folds to use can be specified using the `k_folds` argument. To compare models, we ran this function with the same number of folds specified for each model, then extracted the summed log-likelihood value for each model.

Tanner crab

We utilized abundance and biomass data collected from the NMFS summer bottom trawl survey (1975-2024) to fit Tanner crab models in *sdmTMB*. Sex-size/maturity categories included all males combined, immature females, and mature females, and data were filtered to only include crab with a carapace width greater than or equal to 25mm. As the survey gear and methods were standardized in 1982 (Stauffer 2004), we fit separate models to data before 1982 and data in and after 1982 for each sex-size/maturity category. To evaluate decision points for model formulations, we fit models using a 50-knot, 90-knot, and 120-knot mesh

(Figures 2 - 4), a Tweedie or delta-gamma model family, and a IID spatiotemporal random field. Models fit using the delta-lognormal family did not pass initial model sanity checks and models using an ar1 or random walk spatiotemporal random field did not converge. Therefore, we do not discuss these frameworks any further. The best model framework was used to predict Tanner crab abundance and biomass on an EBS-wide survey grid (Figure 1), a grid encompassing the EBS area west of 166° (for the Tanner West stock; Figure 21, Appendix), and a grid encompassing the EBS area east of 166° (for the Tanner East stock; Figure 22, Appendix). Each prediction grid was a resolution of 5 km².

Norton Sound red king crab

We combined data from the NMFS trawl survey (1976-1991), ADF&G trawl survey (1996-2024), and NMFS NBS trawl survey (2010-2023) into a single data set to which we fit models in *sdmTMB*. We filtered the data set to ensure that it included only observations with coordinates falling within the Norton Sound Section of Statistical Area Q. For model fitting, we used spatial meshes at three resolutions: 100 knots, 50 knots, and 30 knots (Figures ?? - ??). We used a prediction grid with resolution of 5 km² (Figure ??).

St. Matthew Island blue king crab

For model fitting, we used spatial meshes at three resolutions: 120 knots, 90 knots, and 50 knots (Figures ?? - ??). We used a prediction grid with a resolution of 4 km² (Figure ??).

Results

Tanner crab

Model diagnostics

All models passed sanity checks. Model diagnostics using DHARMA residuals varied among the number of knots specified in the mesh (50, 90, 120), model family (Tweedie, delta-gamma), and data period (pre-1982, 1982 onward) for both abundance (Table 1) and biomass (Table 2) models. For male abundance, a model using a delta-gamma distribution and 50 knots performed the best for both periods in terms of the greatest log-likelihood, with only the post-1982 model showing evidence of outliers, zero-inflation, and quantile deviations. However, this was true regardless of the model family or number of knots used. This pattern holds true across other sex-maturity categories. For immature female abundance, a delta-gamma model had the largest log-likelihood across periods, with models using 90 and 50 knots performing best pre-1982 and post-1982, respectively. The best model pre-1982 showed evidence of quantile deviation and dispersion, whereas the best model post-1982 showed evidence of outliers, zero-inflation, and quantile deviation. Contrasting the other two sex-maturity categories, the Tweedie family had the largest log-likelihood for mature female abundance, with 90 and 50 knots performing best pre-1982 and post-1982, respectively. The pre-1982 Tweedie model only showed evidence of zero-inflation, whereas the post-1982 Tweedie model showed evidence of outliers, dispersion, zero-inflation, and quantile deviation.

As with male abundance, a delta-gamma model using 50 knots had the largest log-likelihood for male biomass pre- and post-1982. Models for both periods showed evidence of quantile deviation, dispersion, and outliers, where just the post-1982 model also showed evidence of zero-inflation as was true for other models in this period. For immature female biomass, a Tweedie model using 90 and 50 knots for pre- and post-1982 had the greatest log-likelihood. While the pre-1982 Tweedie model had the largest log-likelihood, it showed evidence of dispersion and zero-inflation whereas the next-best model, a delta-gamma using 90 knots, did not. For immature female biomass post-1982, a Tweedie and delta-gamma model using 50 knots had the largest and very similar log-likelihoods, with the Tweedie model showing evidence of quantile deviation, dispersion, outliers, and zero-inflation where the delta-gamma model did not show evidence of dispersion. A similar pattern was seen in diagnostics for mature female biomass models, where Tweedie models using 50 knots had the largest but very similar log-likelihood values to delta-gamma models using 50 knots across both periods. The pre-1982 50-knot Tweedie model showed evidence of dispersion, outliers, and zero-inflation, whereas

the 50-knot delta-gamma model did not. The post-1982 50-knot Tweedie model exhibited evidence of all diagnostics, whereas the 50-knot delta-gamma model did not show evidence of dispersion.

Accounting for strong model performance across sex-maturity categories, periods, and response (abundance/biomass), we selected the delta-gamma model family and a 50-knot mesh as a parsimonious model framework for prediction. DHARMA residuals for these models across sex-maturity categories and periods did not strongly diverge from the 1-1 line (Figures 5 - 6) despite some evidence of quantile dispersion. In addition, DHARMA residuals for these models did not show evidence of spatiotemporal autocorrelation (Figures 7 - 12).

Predicted abundance and biomass

Heat maps of EBS-wide predicted abundance for Tanner crab males, immature females, and mature females are shown in figures 13 - 15, respectively, using our chosen model framework (delta-gamma, 50 knots). Heat maps of EBS-wide predicted biomass for Tanner crab males, immature females, and mature females are shown in figures 16 - 18. Abundance and biomass heat maps for Tanner crab west and east of 166° are shown in Appendix figures 23 - 28 and figures 29 - 34, respectively.

Predicted index fits to observations

The EBS-wide model-predicted indices varied in their fits to survey abundance (Figure 19) and biomass observations (Figure 20) across sex-maturity categories and between model fitting periods. Across sex-maturity categories, model fits with different knots were most variable before 1982 which could be due to high variability in the spatial footprint of the survey in this period. In this period, uncertainty was generally greater in indices predicted using 50 knots, with the majority of survey observations points and associated uncertainty overlapping with model predicted values and uncertainty. From 1982 onward, indices predicted at different knots are less variable compared with each other, with models using 50 knots generally exhibiting greater uncertainty than 90 and 120 knots. As before, the majority of survey observations points and associated uncertainty overlap with model predicted values and uncertainty across knot specifications. Similar patterns across knots and sex-maturity categories were seen for predicted abundance and biomass indices for Tanners west and east of 166° ()

sdmTMB vs. VAST comparision

Norton Sound red king crab

Model diagnostics

The DHARMA residuals diagnostic plots show evidence of quantile deviations for all three NSRKC models (Figures ?? - ??). The models with 100 knots and 50 knots showed evidence of underdispersion, with observed data less dispersed than expected under the fitted models, while the model with 30 knots did not. None of the models showed evidence of outliers or zero inflation.

Predicted abundance

Heat maps of predicted NSRKC abundance for the three models are show in figures ?? - ??.

St. Matthew Island blue king crab

Model diagnostics

Examination of DHARMA residuals showed similar patterns for the three SMBKC models (Figures ?? - ??). All three models showed evidence of underdispersion, with observed data less dispersed than expected under the fitted models. None of the models showed evidence of outliers. All three models showed evidence of quantile deviations. The model with 120 knots showed evidence of zero inflation, with the observed data containing more zeros than would be expected under the fitted model, but the models with 50 and 90 knots did not show evidence of zero inflation.

Predicted abundance

Heat maps of predicted SMBKC abundance for the three models are show in figures ?? - ??.

Predicted index fits to observations

The model-predicted indices varied in their fits to the survey biomass observations, with the model fit using a mesh with an intermediate number of knots seeming to fit the survey observations more closely than the models fit to meshes with either higher or lower numbers of knots (Figure ??).

Conclusions

Acknowledgements

The authors thank Katie Palof and Mike Litzow for their support and feedback on this work.

References

- Anderson, S.C., Ward, E.J., English, P.A., Barnett, L.A.K. 2022. sdmTMB: An R package for fast, flexible, and user-friendly generalized linear mixed effects models with spatial and spatiotemporal random fields. *bioRxiv*.
- Anderson, S.C., Ward, E.J., English, P.A., Barnett, L.A.K., Thorson, J.T. 2024. Cross-validation for model evaluation and comparison. Retrieved from <https://pbs-assess.github.io/sdmTMB/articles/cross-validation.html>.
- Barbeaux, S.J., L. Barnett, P. Hulson, J. Nielsen, S.K. Shotwell, E. Siddon, I. Spies. 2024. Assessment of the Pacific cod stock in the Eastern Bering Sea. In: Stock Assessment and Fishery Evaluation report for the Groundfish Resources of the Bering Sea/Aleutian Islands regions. North Pacific Fishery Management Council, Anchorage, AK.
- DeFilippo, L., S. Kotwicki, L. Barnett, J. Richar, M.A. Litzow, W.T. Stockhausen, K. Palof. 2023. Evaluating the impacts of reduced sampling density in a systematic fisheries-independent survey design. *Frontiers in Marine Science* 10:1219283.
- Hamazaki, T. 2024. Norton Sound red king crab stock assessment for the fishing year 2024. In: Stock Assessment and Fishery Evaluation Report for the King and Tanner Crab Fisheries of the Bering Sea and Aleutian Islands: 2024 Final Crab SAFE. North Pacific Fishery Management Council, Anchorage AK.
- Hartig, F. 2022. DHARMA: Residual Diagnostics for Hierarchical (Multi-Level / Mixed) Regression Models. R package version 0.4.6, <https://CRAN.R-project.org/package=DHARMA>.
- Ianelli, J., D. Webber, J. Zheng, A. Letaw. 2017. Saint Matthew Island blue king crab stock assessment 2017. In: Stock Assessment and Fishery Evaluation Report for the King and Tanner Crab Fisheries of the Bering Sea and Aleutian Islands: 2017 Final Crab SAFE. North Pacific Fishery Management Council, Anchorage AK.
- Ianelli, J., T. Honkalehto, S. Wassermann, A. McCarthy, S. Steinessen, C. McGilliard, E. Siddon. 2024. Assessment of walleye pollock in the eastern Bering Sea. In: Stock Assessment and Fishery Evaluation report for the Groundfish Resources of the Bering Sea/Aleutian Islands regions. North Pacific Fishery Management Council, Anchorage, AK.
- SSC. 2017. Scientific and Statistical Committee report to the North Pacific Fishery Management Council, October 2nd-4th, 2017. North Pacific Fishery Management Council, Anchorage, AK.
- Stauffer, G.A. 2004. NOAA protocols for groundfish bottom trawl surveys of the Nation's fishery resources. U.S. Dep. Commer., NOAA Tech. Memo. NMFS-F/SPO-65, 205p.
- Stern, C., K. Palof. 2024. Saint Matthew Island blue king crab stock assessment 2024. In: Stock Assessment and Fishery Evaluation Report for the King and Tanner Crab Fisheries of the Bering Sea and Aleutian Islands: 2024 Final Crab SAFE. North Pacific Fishery Management Council, Anchorage AK.
- Stockhausen, W.T. 2024. 2024 stock assessment and fishery evaluation report for the Tanner crab fisheries of the Bering Sea and Aleutians Islands regions. In: Stock Assessment and Fishery Evaluation Report for the King and Tanner Crab Fisheries of the Bering Sea and Aleutian Islands: 2024 Final Crab SAFE. North Pacific Fishery Management Council, Anchorage AK.
- Thorson, J.T. 2019. Guidance for decisions using the vector autoregressive spatio-temporal (VAST) package in stock, ecosystem, habitat, and climate assessments. *Fisheries Research* 210:143-161. <https://doi.org/10.1016/j.fishres.2018.10.013>
- Yalcin, S., S.C. Anderson, P.M. Regular, P.A. English. 2023. Exploring the limits of spatiotemporal and design-based index standardization under reduced survey coverage. *ICES Journal of Marine Sciences* 80:2368-2379. <https://doi.org/10.1093/icesjms/fsad155>

Tables

Table 1: Tanner crab diagnostic values for abundance models fit with Tweedie or delta gamma families and a spatial resolution of 50, 90, or 120 knots across sex-size maturity categories and model-fitting periods (pre-1982, during or after 1982). Log-likelihood values were estimated using the cross-validation function in sdmTMB with 3 folds. Quantile, dispersion, outlier, and zero-inflation diagnostics were estimated from DHARMA residuals, with values below 0.05 indicating significant metrics. Values are ordered within sex-size maturity category and period by decreasing log-likelihood.

Category	Period	Family	Knots	Log-likelihood	Quantiles	Dispersion	Outliers	Zero-inflation
Immature Female	<1982	Delta-gamma	90	-6371.5	0.0	0.0	0.5	0.5
Immature Female	<1982	Tweedie	90	-6475.4	0.0	0.0	0.0	0.1
Immature Female	<1982	Tweedie	120	-6666.0	0.1	0.0	0.4	0.2
Immature Female	<1982	Delta-gamma	50	-6716.3	0.0	0.2	0.2	0.0
Immature Female	<1982	Tweedie	50	-6850.9	0.1	0.0	0.1	0.1
Immature Female	<1982	Delta-gamma	120	-6907.8	0.0	0.0	0.1	0.1
Immature Female	>=1982	Delta-gamma	50	-53281.6	0.0	0.1	0.0	0.0
Immature Female	>=1982	Tweedie	50	-53380.1	0.0	0.0	0.0	0.0
Immature Female	>=1982	Tweedie	90	-53543.3	0.0	0.0	0.0	0.0
Immature Female	>=1982	Delta-gamma	90	-53553.8	0.0	0.2	0.0	0.0
Immature Female	>=1982	Tweedie	120	-53722.7	0.0	0.0	0.0	0.0
Immature Female	>=1982	Delta-gamma	120	-53852.8	0.0	0.7	0.0	0.0
Male	<1982	Delta-gamma	50	-9256.2	0.4	0.5	0.1	0.4
Male	<1982	Tweedie	90	-9339.9	0.0	0.0	0.0	0.1
Male	<1982	Delta-gamma	90	-9349.7	0.0	0.1	0.5	0.3
Male	<1982	Tweedie	120	-9397.7	0.0	0.0	0.0	0.0
Male	<1982	Delta-gamma	120	-9398.7	0.1	0.5	0.4	0.1
Male	<1982	Tweedie	50	-9540.7	0.0	0.0	0.0	0.0
Male	>=1982	Delta-gamma	50	-76006.3	0.0	0.1	0.0	0.0
Male	>=1982	Tweedie	50	-76072.9	0.0	0.0	0.0	0.0
Male	>=1982	Tweedie	90	-76229.4	0.0	0.0	0.0	0.0
Male	>=1982	Delta-gamma	90	-76277.7	0.0	0.1	0.0	0.0
Male	>=1982	Tweedie	120	-76318.2	0.0	0.0	0.0	0.0
Male	>=1982	Delta-gamma	120	-76509.5	0.0	0.1	0.0	0.0
Mature Female	<1982	Tweedie	90	-6089.8	0.1	0.4	0.1	0.0
Mature Female	<1982	Delta-gamma	90	-6097.3	0.0	0.8	0.5	0.6
Mature Female	<1982	Delta-gamma	50	-6097.4	0.0	0.4	0.0	0.0
Mature Female	<1982	Delta-gamma	120	-6108.3	0.2	0.3	0.1	0.0
Mature Female	<1982	Tweedie	120	-6132.7	0.0	0.0	0.8	0.0
Mature Female	<1982	Tweedie	50	-6189.4	0.1	0.0	0.0	0.0
Mature Female	>=1982	Tweedie	50	-43560.9	0.0	0.0	0.0	0.0
Mature Female	>=1982	Delta-gamma	50	-43625.4	0.0	0.0	0.0	0.0
Mature Female	>=1982	Delta-gamma	90	-43803.8	0.0	0.0	0.0	0.0
Mature Female	>=1982	Delta-gamma	120	-43943.3	0.0	0.0	0.0	0.0
Mature Female	>=1982	Tweedie	90	-43837.0	0.0	0.0	0.0	0.0
Mature Female	>=1982	Tweedie	120	-44059.6	0.0	0.0	0.0	0.0

Table 2: Tanner crab diagnostic values for biomass models fit with Tweedie or delta gamma families and a spatial resolution of 50, 90, or 120 knots across sex-size maturity categories and model-fitting periods (pre-1982, during or after 1982). Log-likelihood values were estimated using the cross-validation function in sdmTMB with 3 folds. Quantile, dispersion, outlier, and zero-inflation diagnostics were estimated from DHARMA residuals, with values below 0.05 indicating significant metrics. Values are ordered within sex-size maturity category and period by decreasing log-likelihood.

Category	Period	Family	Knots	Log-likelihood	Quantiles	Dispersion	Outliers	Zero-inflation
Immature Female	<1982	Tweedie	90	-6356.8	0.2	0.0	1.0	0.0
Immature Female	<1982	Delta-gamma	90	-6514.3	0.1	0.3	0.4	0.1
Immature Female	<1982	Delta-gamma	120	-6630.5	0.0	0.1	0.9	0.3
Immature Female	<1982	Tweedie	120	-6823.7	0.1	0.1	0.7	0.8
Immature Female	<1982	Delta-gamma	50	-6874.7	0.0	0.0	0.0	0.0
Immature Female	<1982	Tweedie	50	-7246.5	0.0	0.0	0.2	0.3
Immature Female	>=1982	Tweedie	50	-53292.8	0.0	0.0	0.0	0.0
Immature Female	>=1982	Delta-gamma	50	-53303.1	0.0	0.1	0.0	0.0
Immature Female	>=1982	Tweedie	90	-53587.3	0.0	0.0	0.0	0.0
Immature Female	>=1982	Delta-gamma	120	-53639.8	0.0	1.0	0.0	0.0
Immature Female	>=1982	Tweedie	120	-53652.8	0.0	0.0	0.0	0.0
Immature Female	>=1982	Delta-gamma	90	-53652.9	0.0	0.9	0.0	0.0
Male	<1982	Delta-gamma	50	-9275.5	0.0	0.0	0.0	0.3
Male	<1982	Tweedie	90	-9295.3	0.0	0.0	0.1	0.3
Male	<1982	Tweedie	50	-9309.6	0.0	0.0	0.0	0.1
Male	<1982	Delta-gamma	120	-9343.0	0.0	0.0	0.1	0.7
Male	<1982	Delta-gamma	90	-9349.5	0.0	0.0	0.4	0.0
Male	<1982	Tweedie	120	-9422.2	0.0	0.0	0.5	0.6
Male	>=1982	Delta-gamma	50	-75992.4	0.0	0.0	0.0	0.0
Male	>=1982	Tweedie	50	-76031.1	0.0	0.0	0.0	0.0
Male	>=1982	Delta-gamma	90	-76307.0	0.0	0.0	0.0	0.0
Male	>=1982	Tweedie	120	-76345.7	0.0	0.0	0.0	0.0
Male	>=1982	Delta-gamma	120	-76382.0	0.0	0.0	0.0	0.0
Male	>=1982	Tweedie	90	-76489.4	0.0	0.0	0.0	0.0
Mature Female	<1982	Tweedie	50	-6101.9	0.2	0.0	0.0	0.0
Mature Female	<1982	Delta-gamma	50	-6108.2	0.2	0.1	0.1	0.5
Mature Female	<1982	Delta-gamma	120	-6108.8	0.0	0.4	0.4	0.4
Mature Female	<1982	Delta-gamma	90	-6134.0	0.0	0.3	0.4	0.6
Mature Female	<1982	Tweedie	90	-6135.2	0.2	0.9	0.5	0.0
Mature Female	<1982	Tweedie	120	-6159.8	0.2	0.1	0.0	0.0
Mature Female	>=1982	Tweedie	50	-43735.8	0.0	0.0	0.0	0.0
Mature Female	>=1982	Delta-gamma	90	-43746.8	0.0	0.1	0.0	0.0
Mature Female	>=1982	Tweedie	90	-43818.5	0.0	0.0	0.0	0.0
Mature Female	>=1982	Delta-gamma	50	-43898.4	0.0	0.3	0.0	0.0
Mature Female	>=1982	Delta-gamma	120	-44076.4	0.0	0.0	0.0	0.0
Mature Female	>=1982	Tweedie	120	-44166.4	0.0	0.0	0.0	0.0

Figures

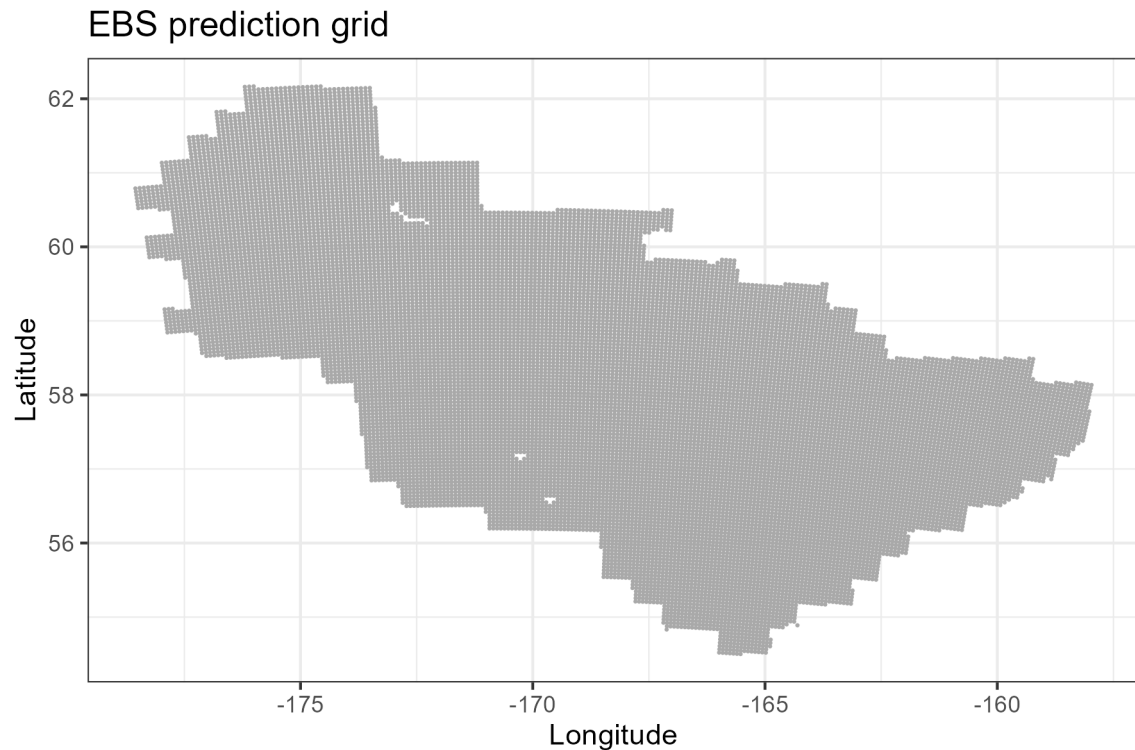
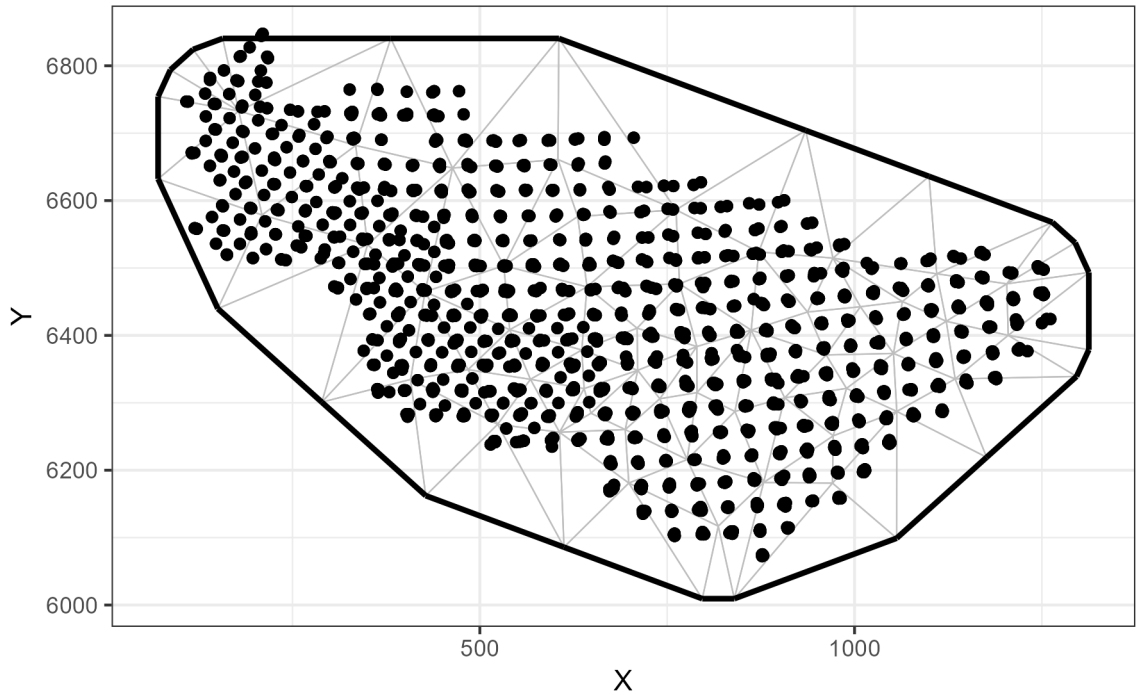


Figure 1: Eastern Bering Sea prediction grid used for Tanner crab spatial abundance and biomass predictions. Spatial resolution is 5km² and does not include land.

<1982 mesh (knots=72)



\geq 1982 mesh (knots=74)

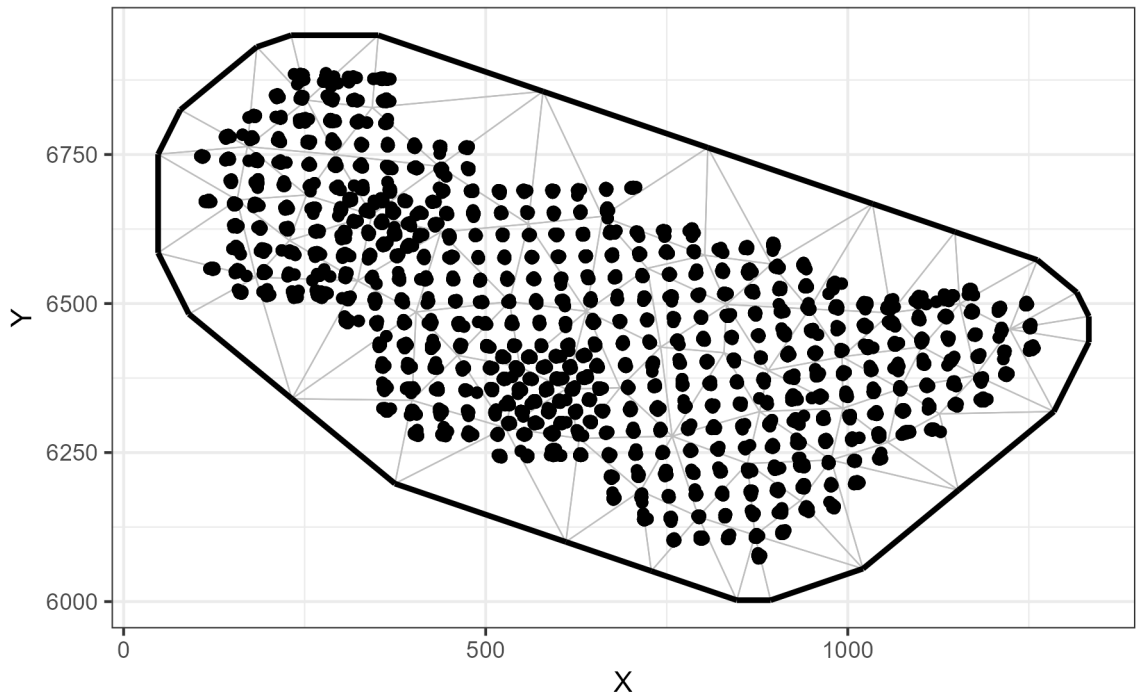
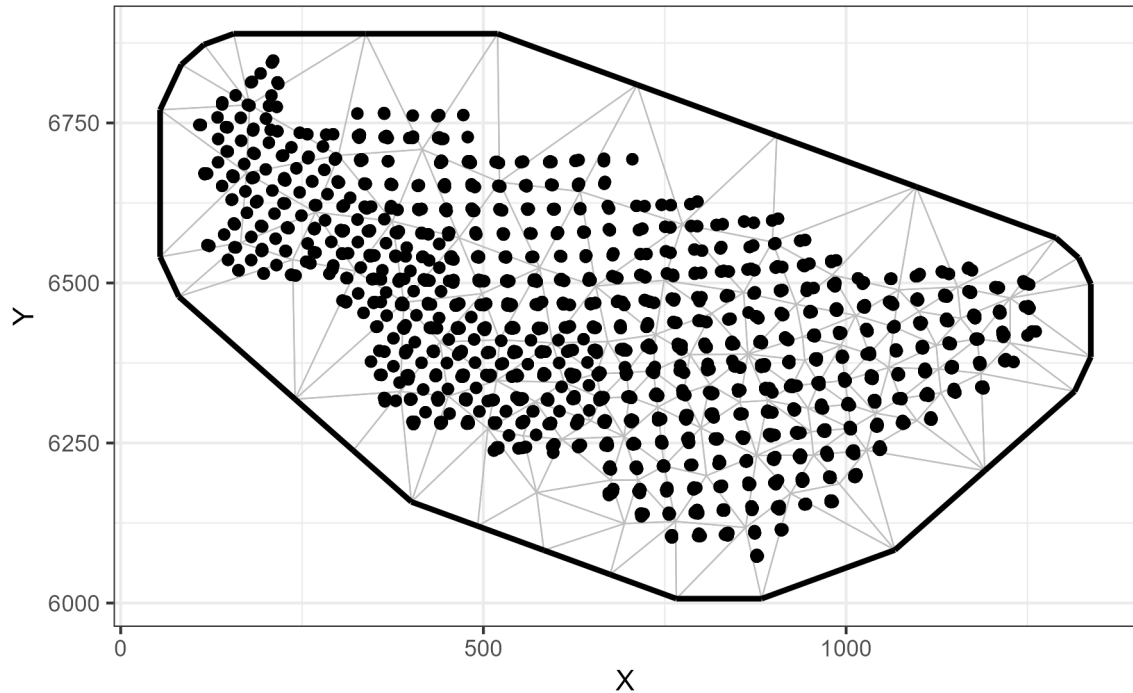


Figure 2: Spatial mesh with 50 knots used for fitting Tanner crab spatial models. Points represent observations and vertices represent knot locations.

<1982 mesh (knots=122)



\geq 1982 mesh (knots=122)

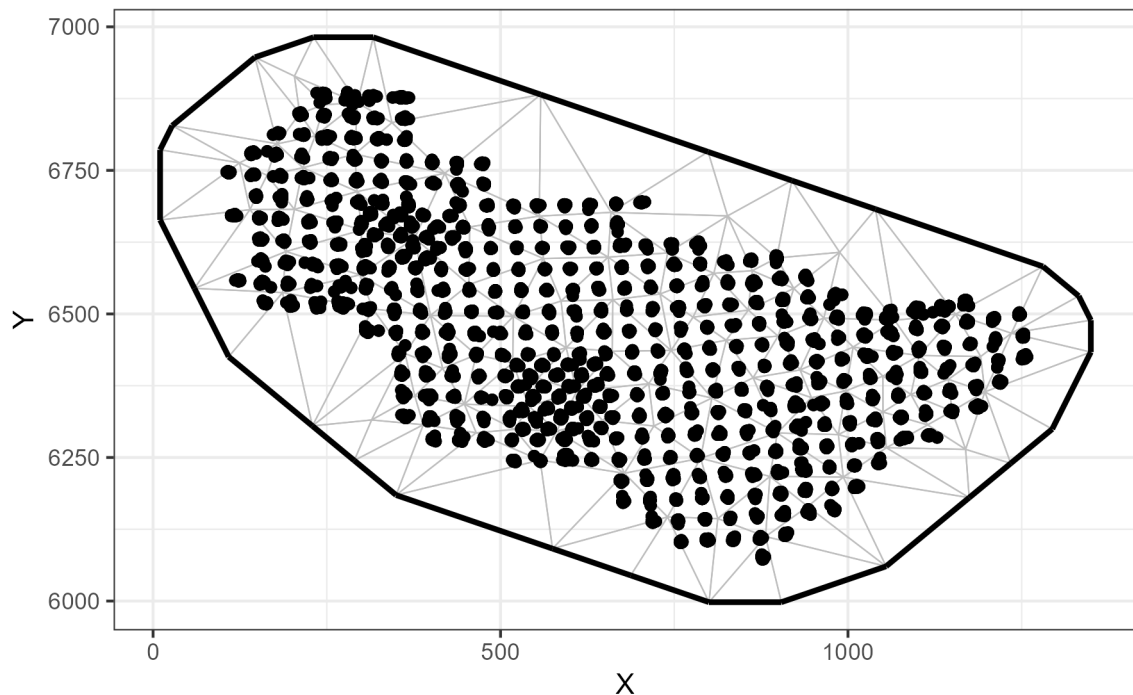


Figure 3: Spatial mesh with 90 knots used for fitting Tanner crab spatial models. Points represent observations and vertices represent knot locations.

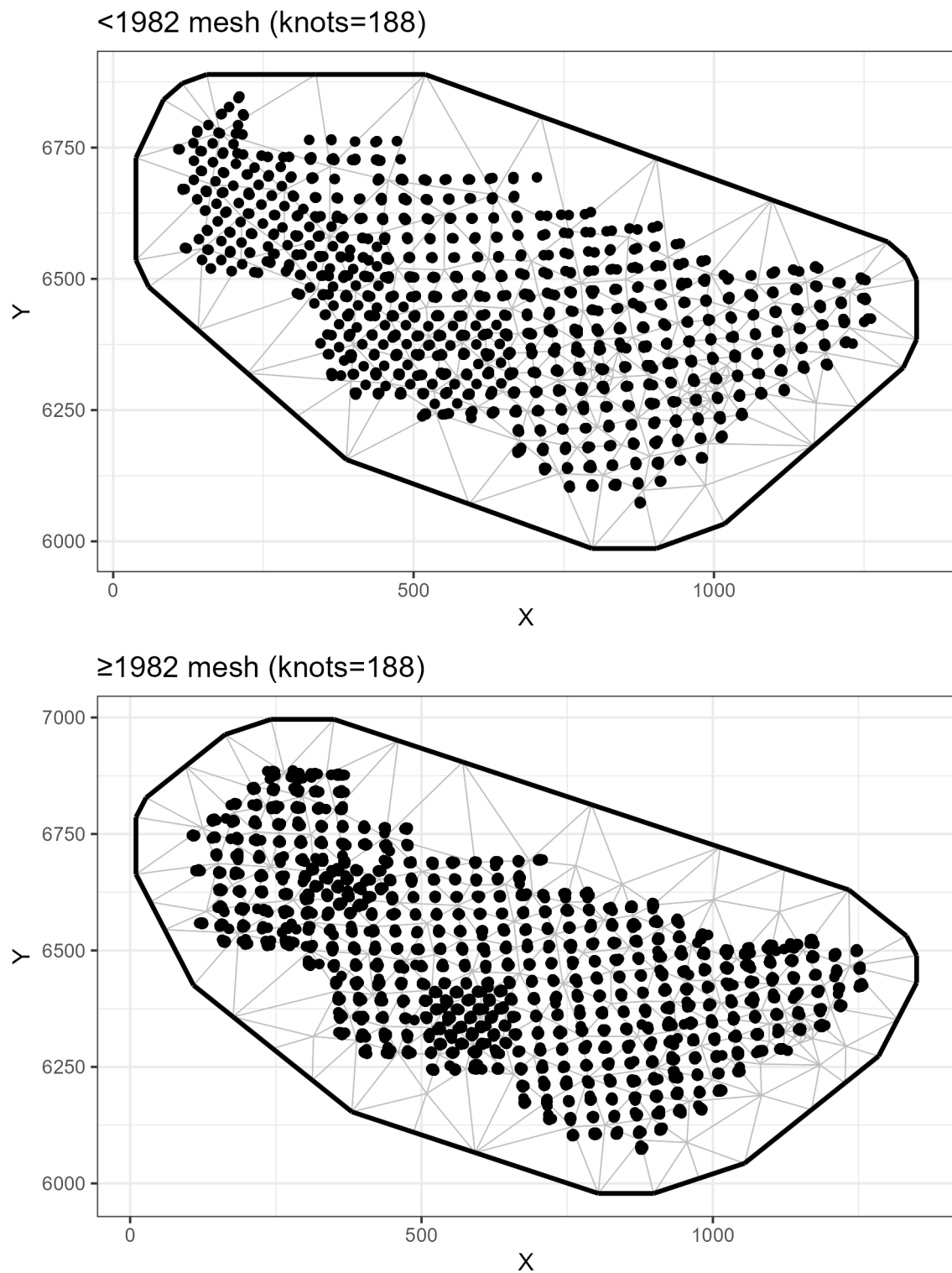


Figure 4: Spatial mesh with 120 knots used for fitting Tanner crab spatial models. Points represent observations and vertices represent knot locations.

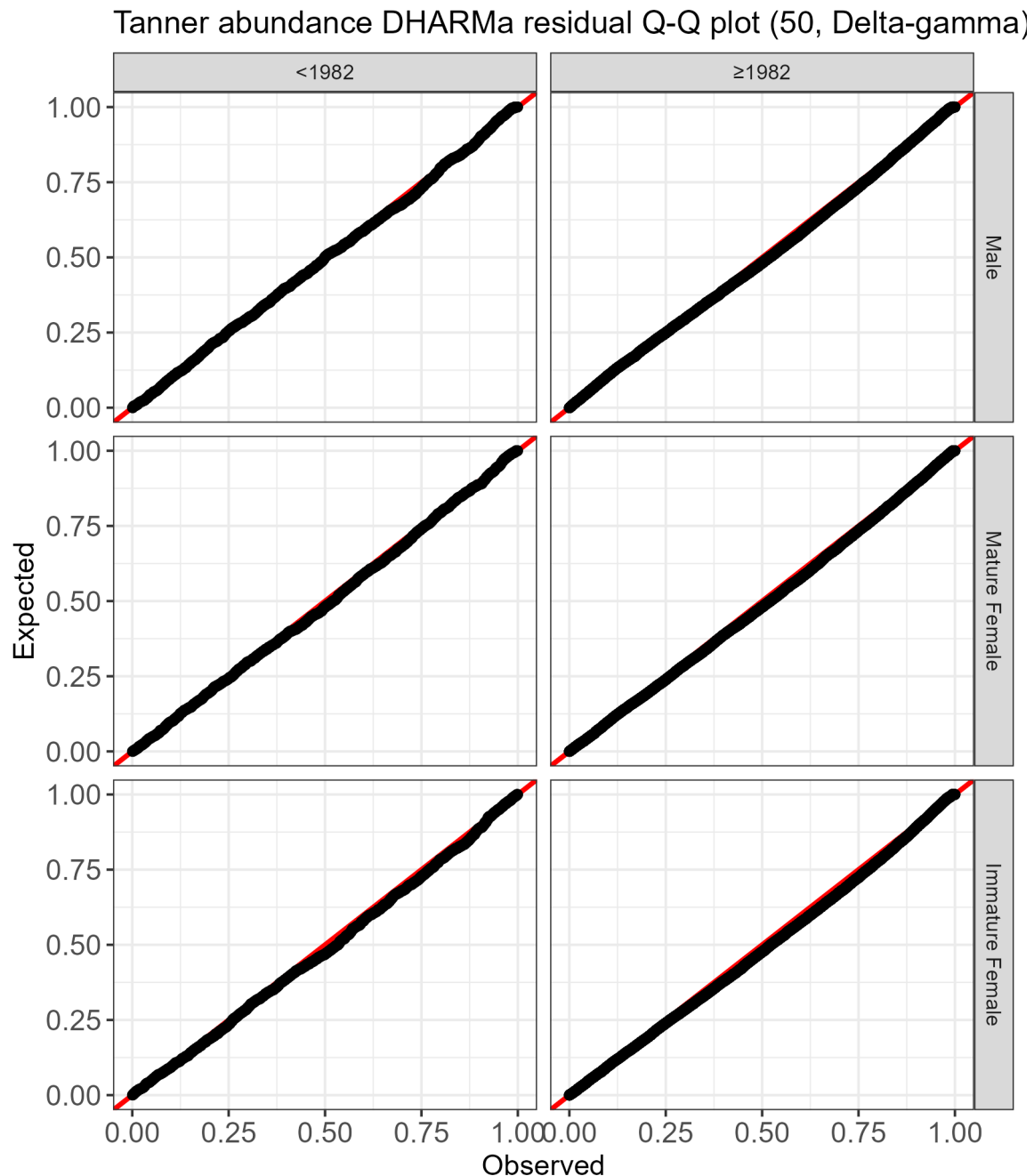


Figure 5: Q-Q plot of DHARMA residuals for abundance models fit with NMFS summer bottom trawl survey data before 1982 (left) and 1982 onward (right) using a delta-gamma model family and 50 knots in the model mesh.

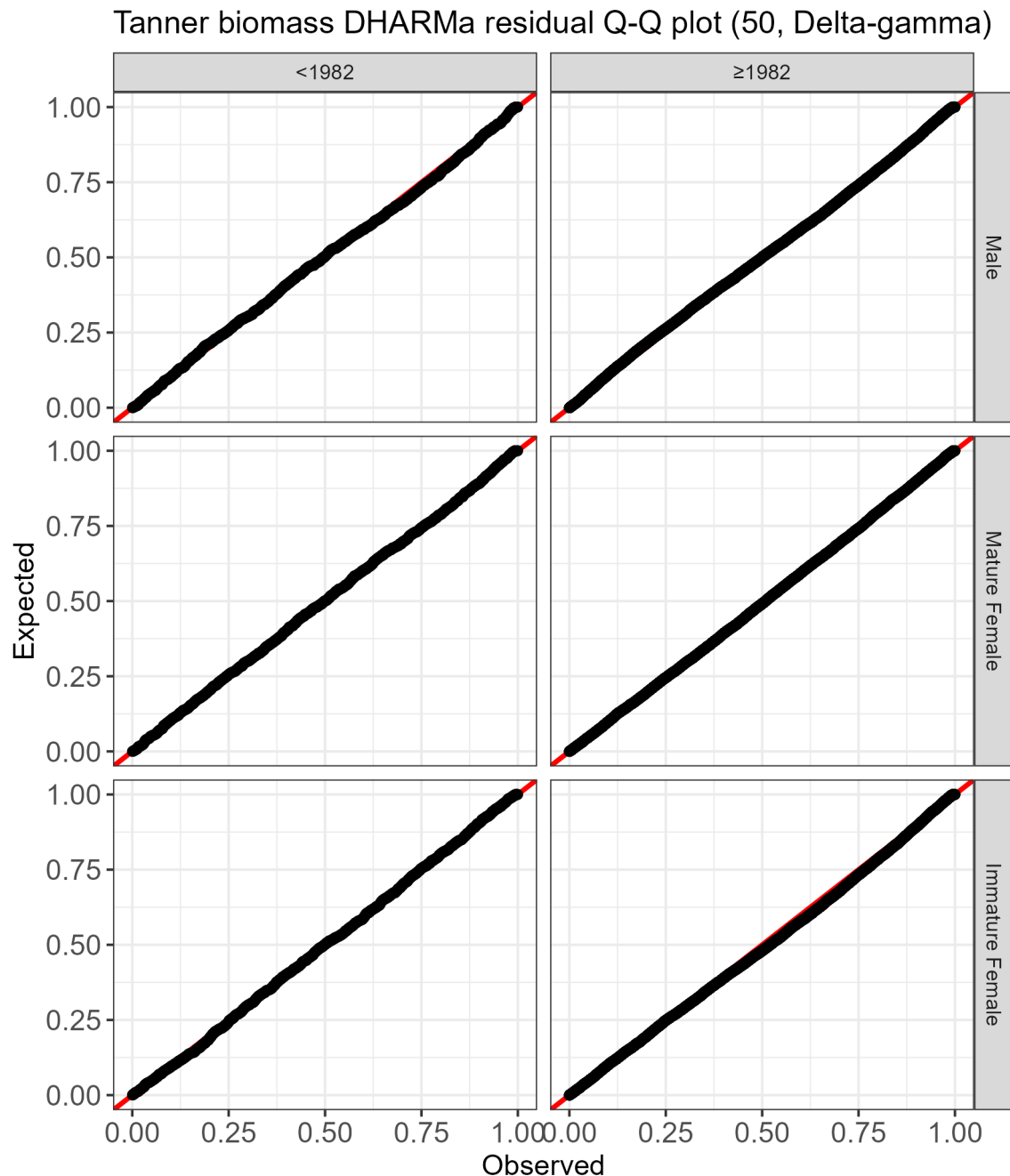


Figure 6: Q-Q plot of DHARMA residuals for biomass models fit with NMFS summer bottom trawl survey data before 1982 (left) and 1982 onward (right) using a delta-gamma model family and 50 knots in the model mesh.

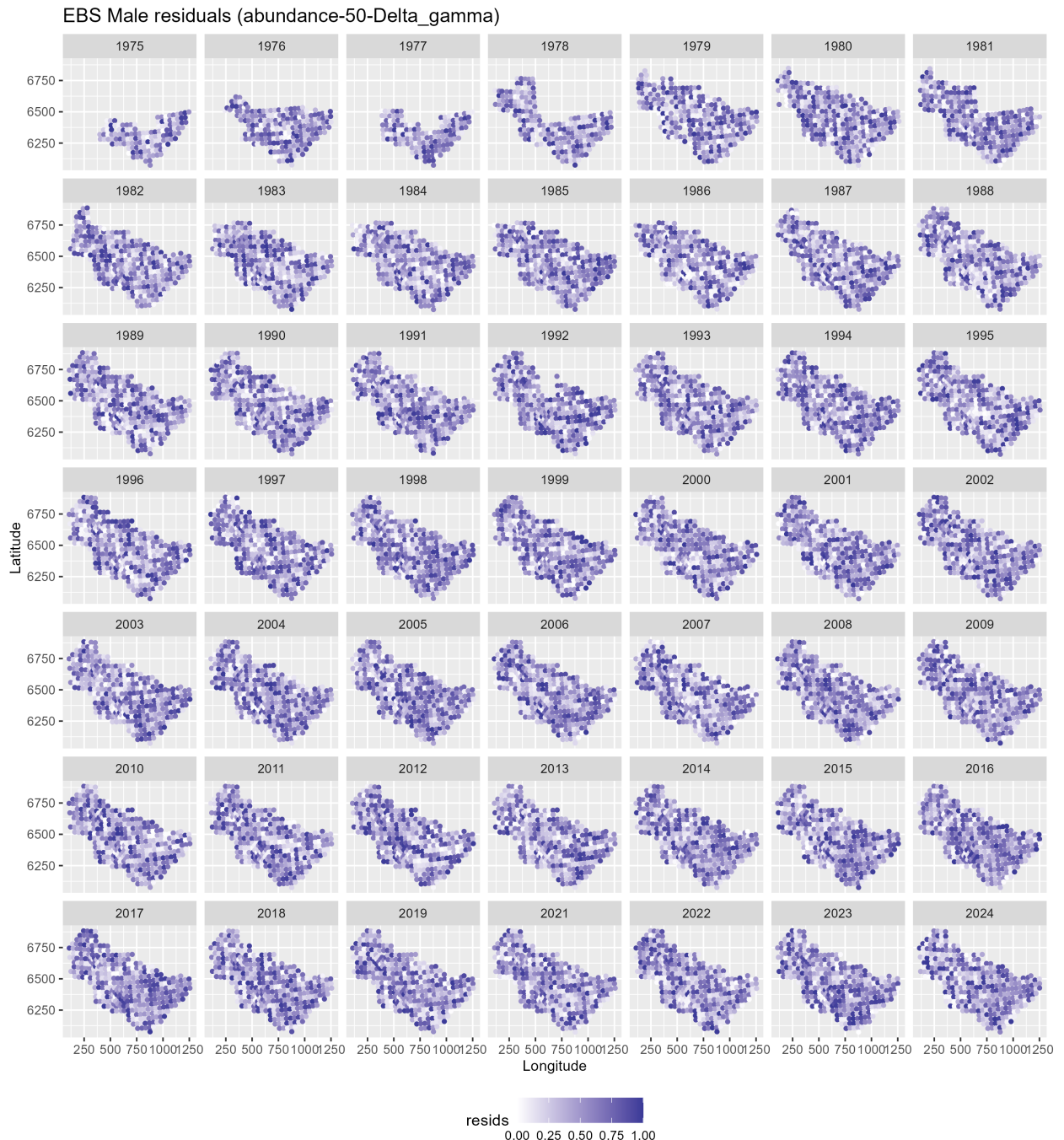


Figure 7: Spatial plot of DHARMA residuals for male abundance models fit using NMFS summer bottom trawl survey data before 1982 and 1982 onward with a 50-knot mesh and a delta-gamma model family. Predictions from both of these periods/models are combined in this figure.

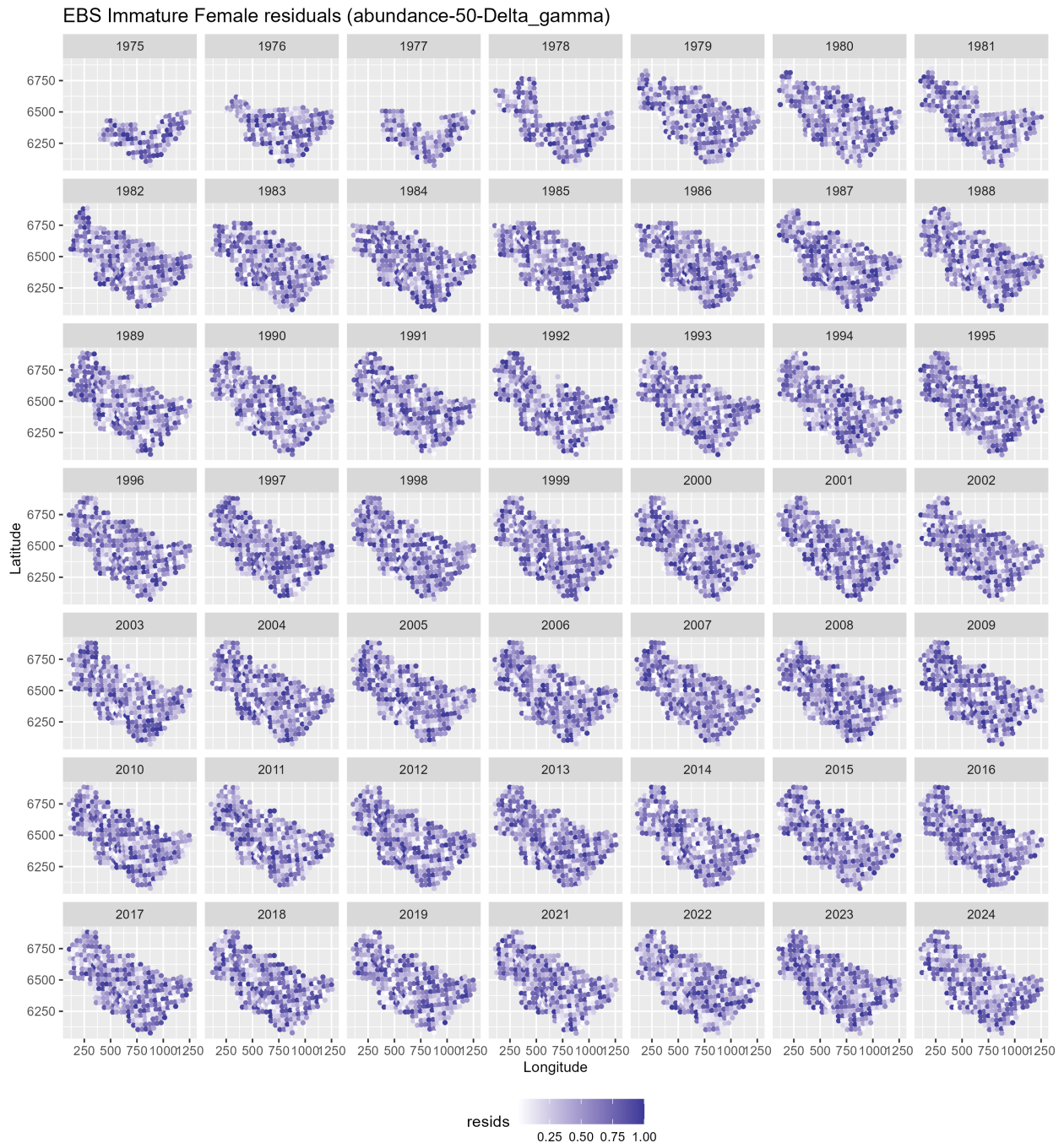


Figure 8: Spatial plot of DHARMA residuals for immature female abundance models fit using NMFS summer bottom trawl survey data before 1982 and 1982 onward with a 50-knot mesh and a delta-gamma model family. Predictions from both of these periods/models are combined in this figure.

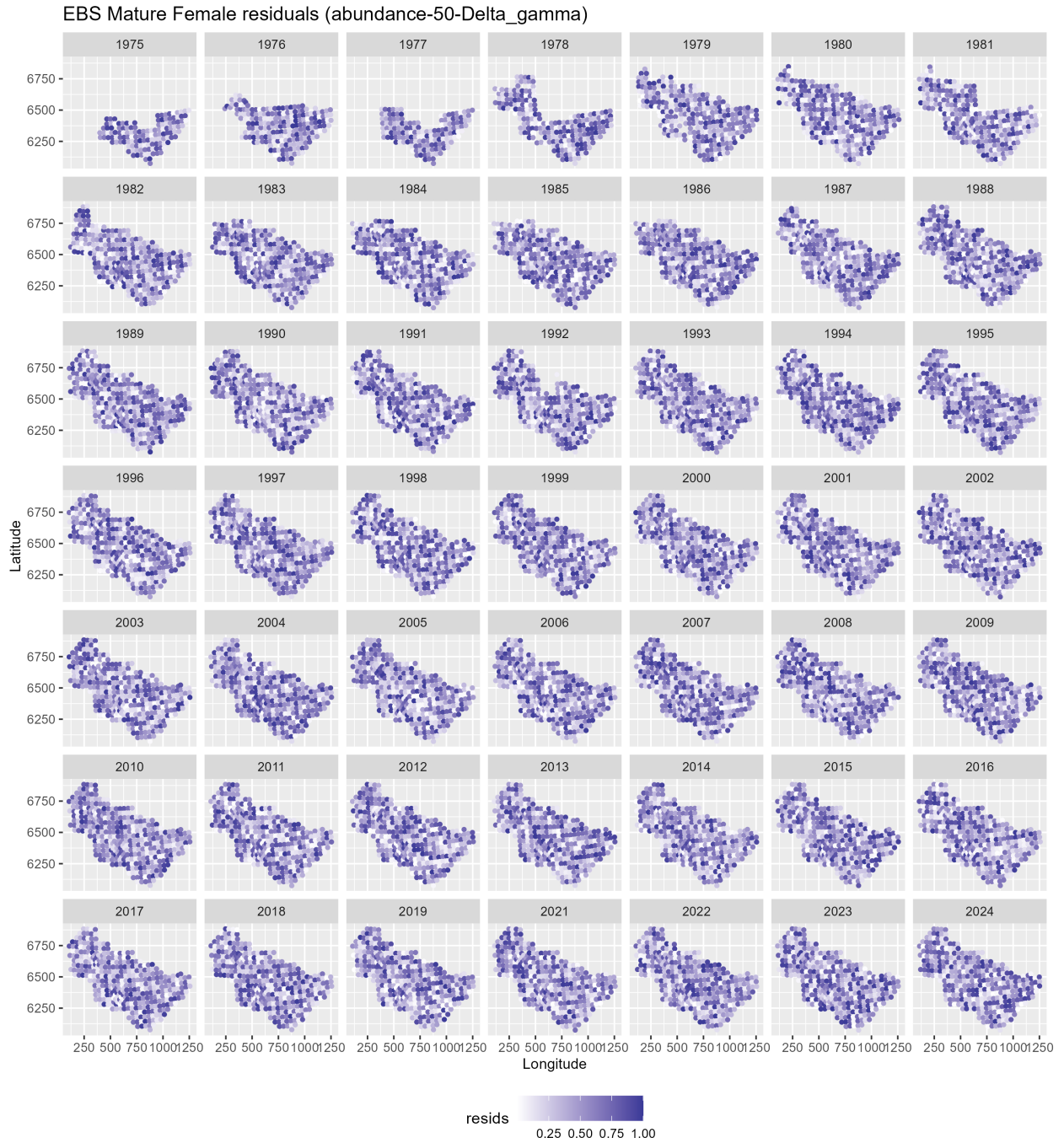


Figure 9: Spatial plot of DHARMa residuals for mature female abundance models fit using NMFS summer bottom trawl survey data before 1982 and 1982 onward with a 50-knot mesh and a delta-gamma model family. Predictions from both of these periods/models are combined in this figure.

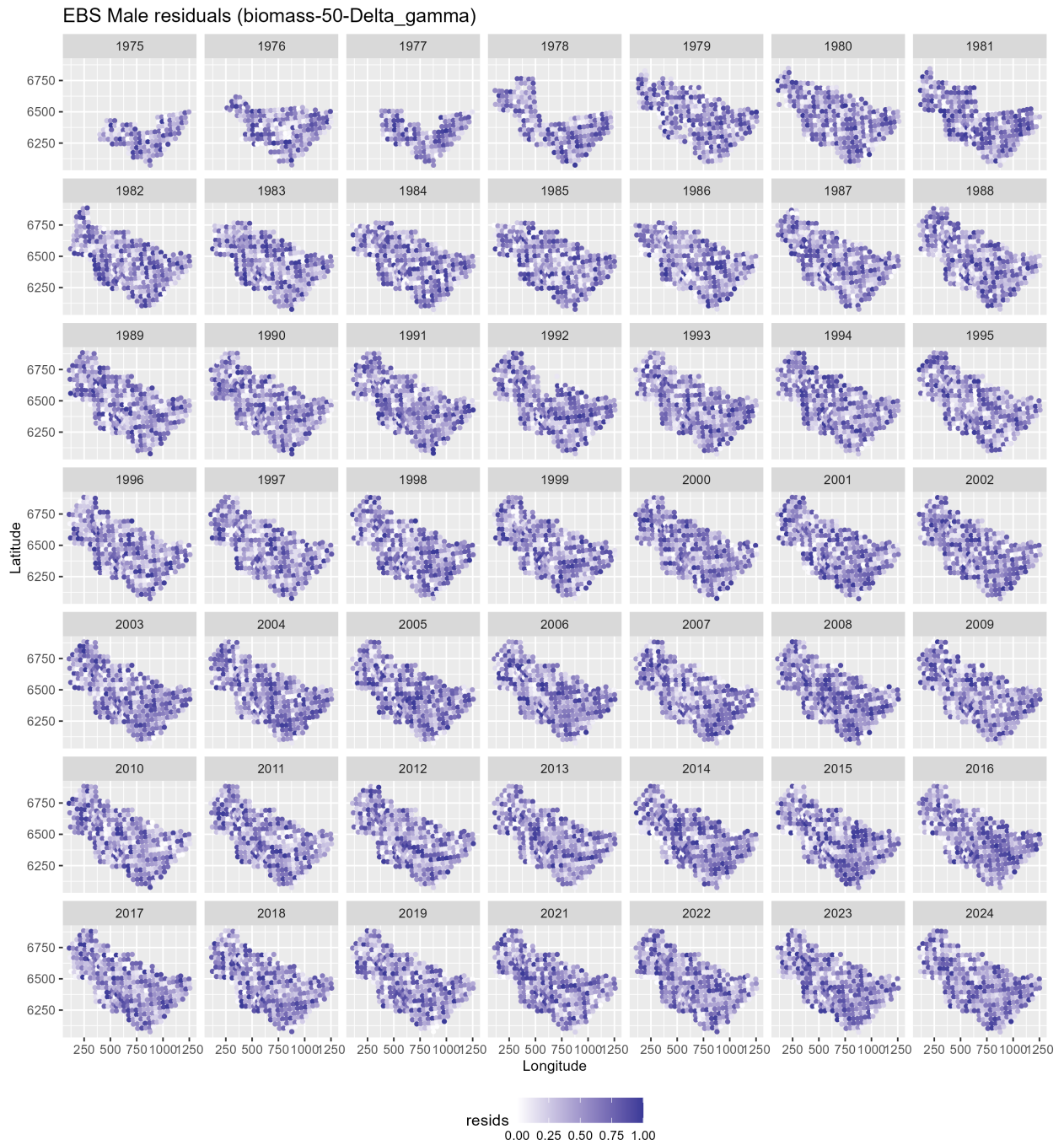


Figure 10: Spatial plot of DHARMA residuals for male biomass models fit using NMFS summer bottom trawl survey data before 1982 and 1982 onward with a 50-knot mesh and a delta-gamma model family. Predictions from both of these periods/models are combined in this figure.

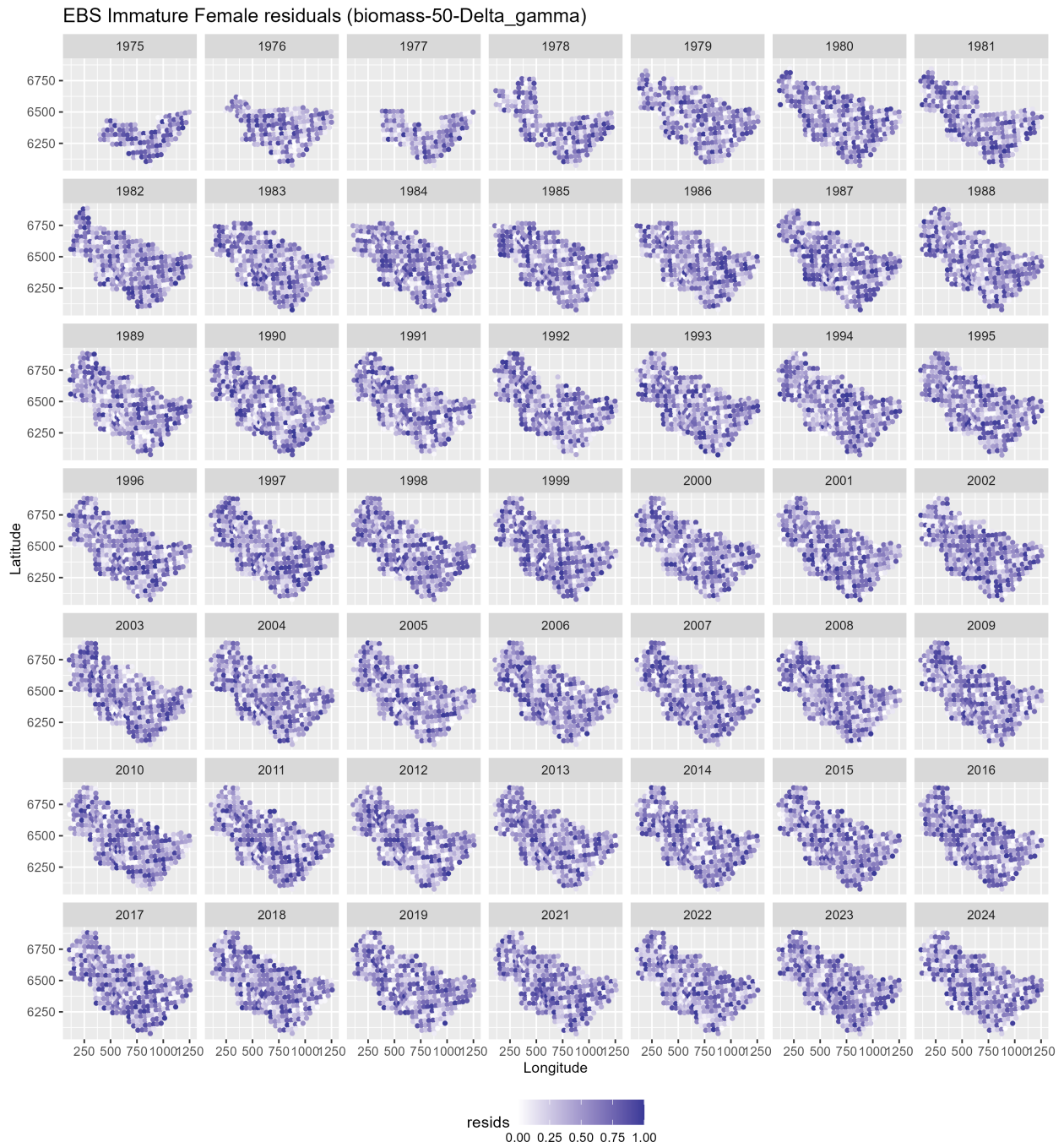


Figure 11: Spatial plot of DHARMA residuals for immature female biomass models fit using NMFS summer bottom trawl survey data before 1982 and 1982 onward with a 50-knot mesh and a delta-gamma model family. Predictions from both of these periods/models are combined in this figure.

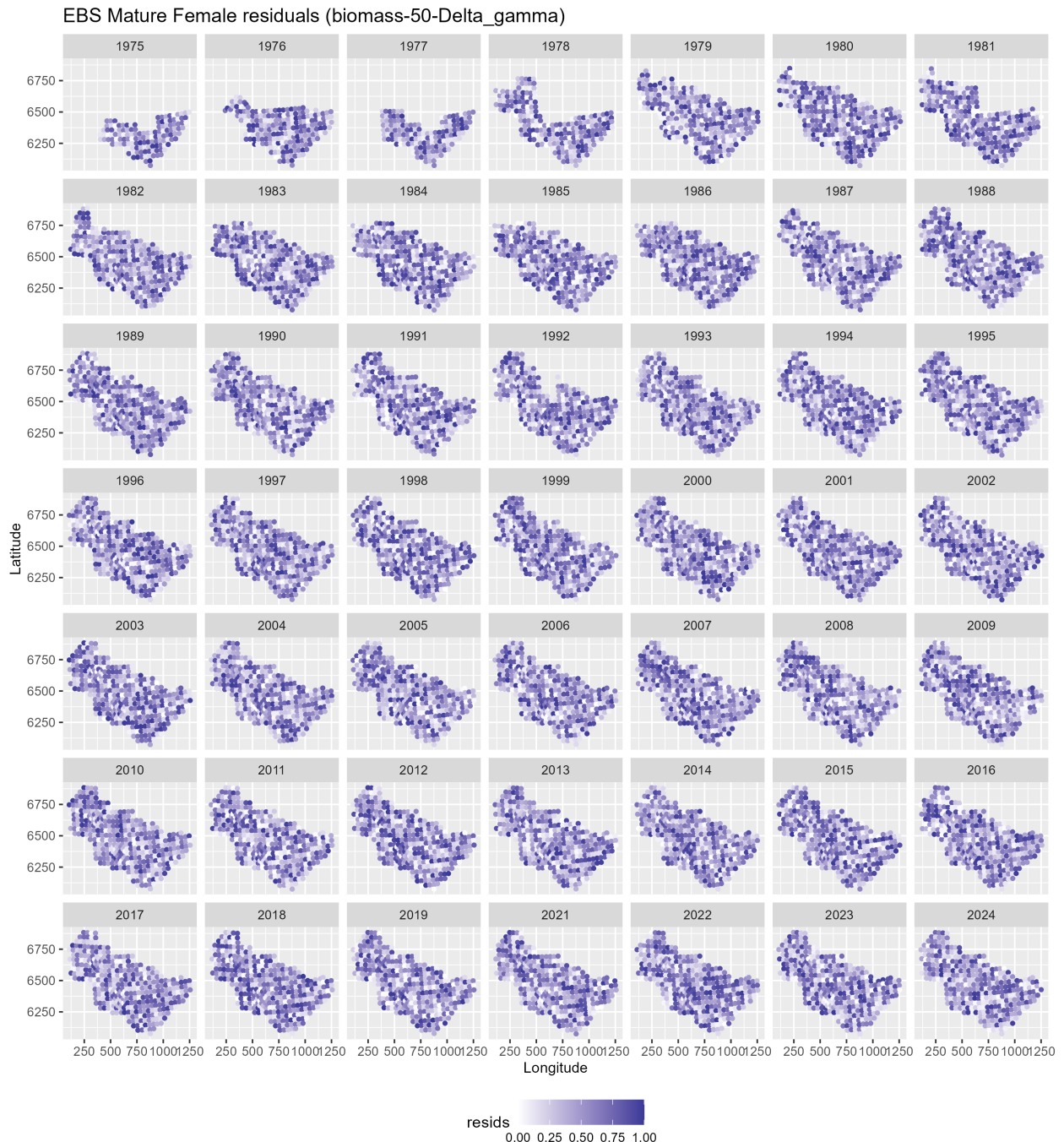


Figure 12: Spatial plot of DHARMA residuals for mature female biomass models fit using NMFS summer bottom trawl survey data before 1982 and 1982 onward with a 50-knot mesh and a delta-gamma model family. Predictions from both of these periods/models are combined in this figure.

EBS predicted male abundance

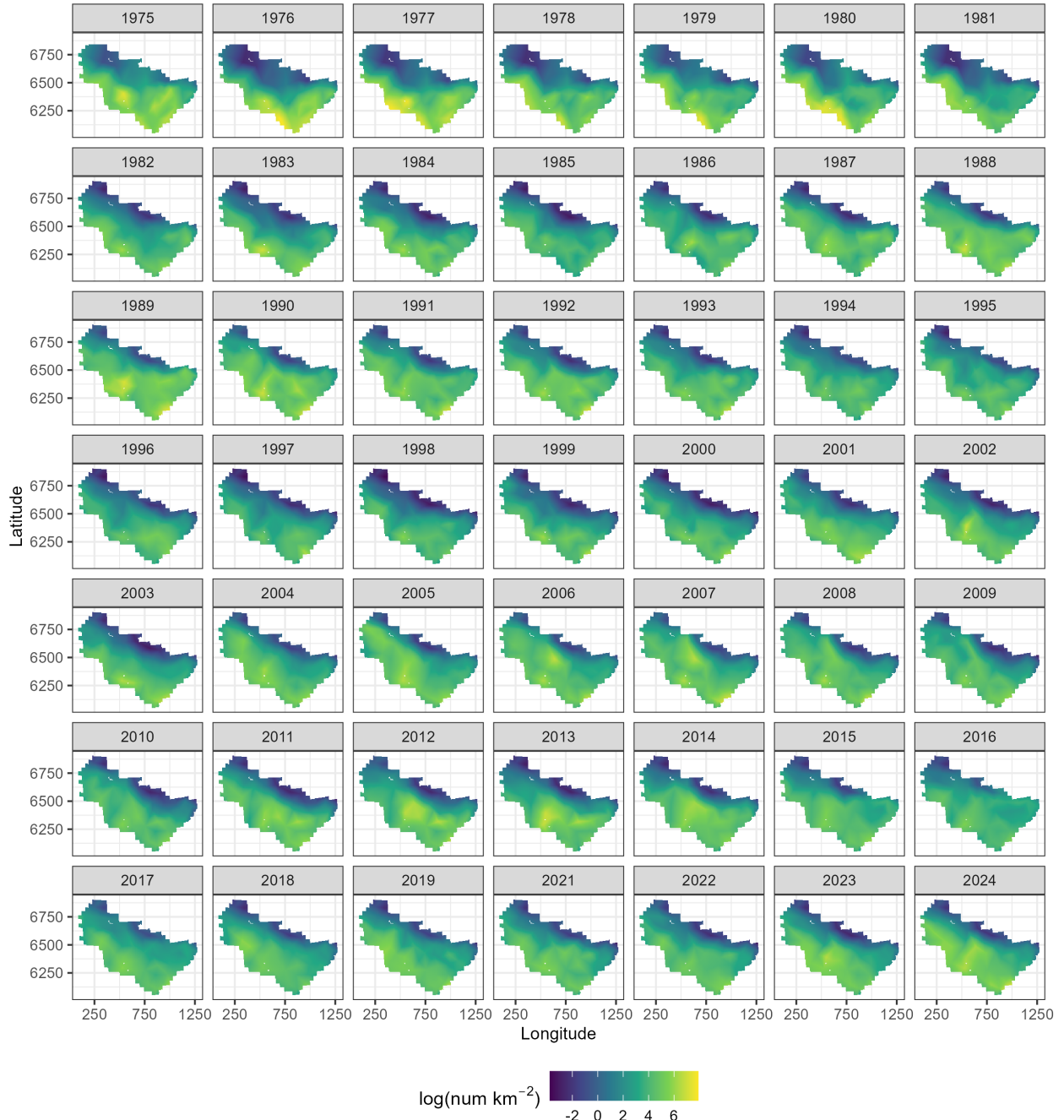


Figure 13: Spatial predictions of male abundance across the Eastern Bering Sea using NMFS summer bottom trawl survey data before 1982 and 1982 onward with a 50-knot mesh and a delta-gamma model family. Predictions from both of these periods/models are combined in this figure.

EBS predicted immature female abundance

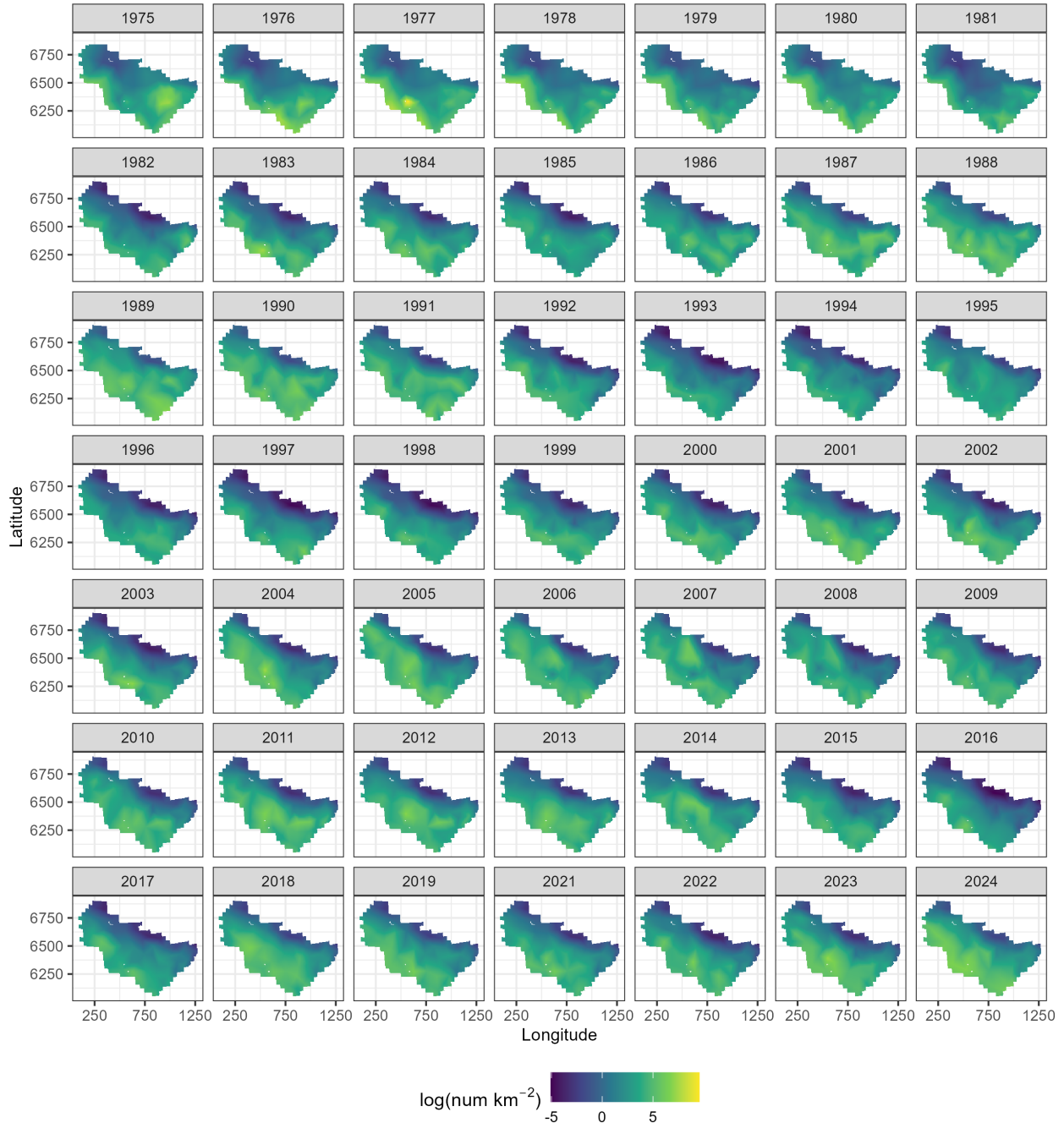


Figure 14: Spatial predictions of immature female abundance across the Eastern Bering Sea using NMFS summer bottom trawl survey data before 1982 and 1982 onward with a 50-knot mesh and a delta-gamma model family. Predictions from both of these periods/models are combined in this figure.

EBS predicted mature female abundance

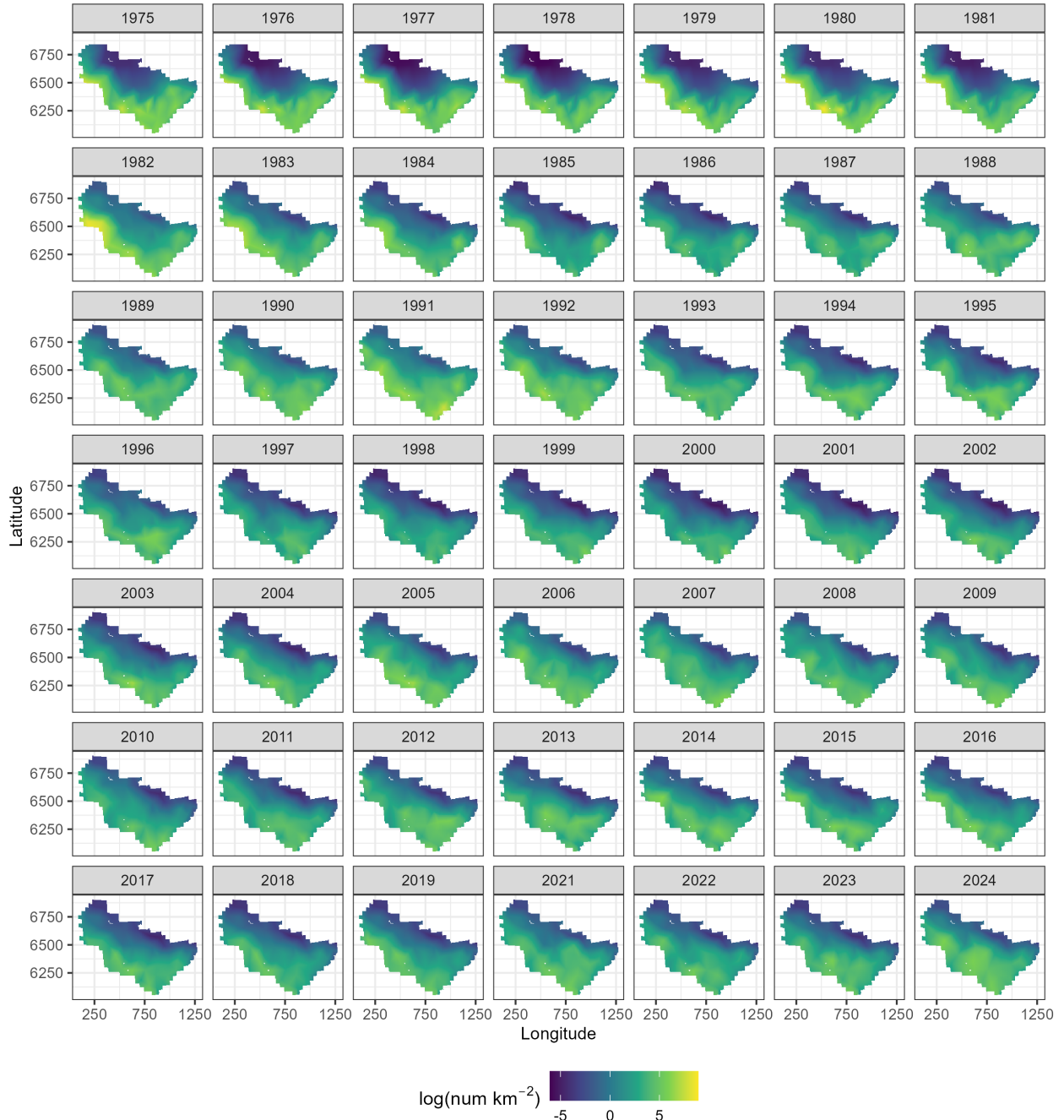


Figure 15: Spatial predictions of mature female abundance across the Eastern Bering Sea using NMFS summer bottom trawl survey data before 1982 and 1982 onward with a 50-knot mesh and a delta-gamma model family. Predictions from both of these periods/models are combined in this figure.

EBS predicted male biomass

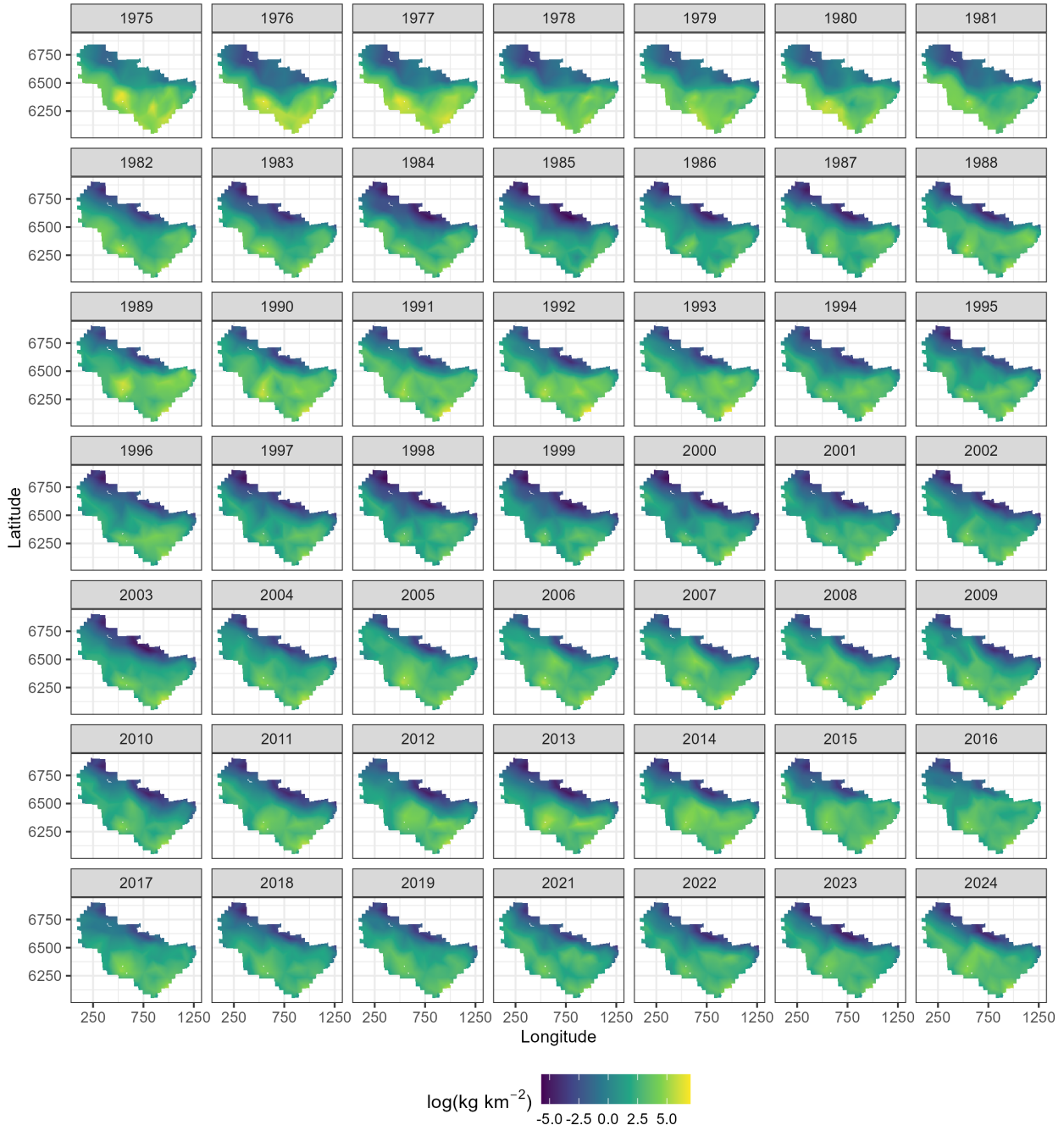


Figure 16: Spatial predictions of male biomass across the Eastern Bering Sea using NMFS summer bottom trawl survey data before 1982 and 1982 onward with a 50-knot mesh and a delta-gamma model family. Predictions from both of these periods/models are combined in this figure.

EBS predicted immature female biomass

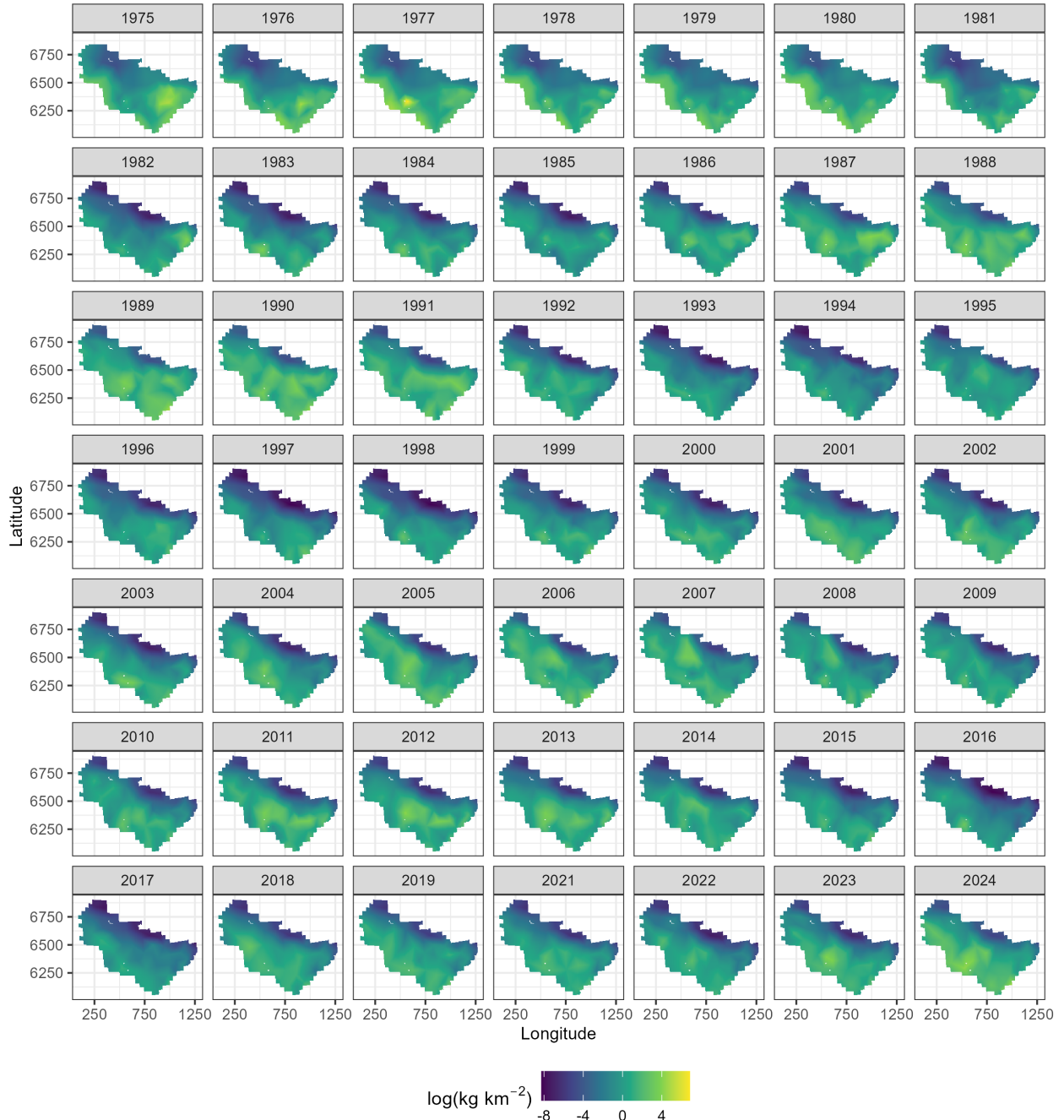


Figure 17: Spatial predictions of immature female biomass across the Eastern Bering Sea using NMFS summer bottom trawl survey data before 1982 and 1982 onward with a 50-knot mesh and a delta-gamma model family. Predictions from both of these periods/models are combined in this figure.

EBS predicted mature female biomass

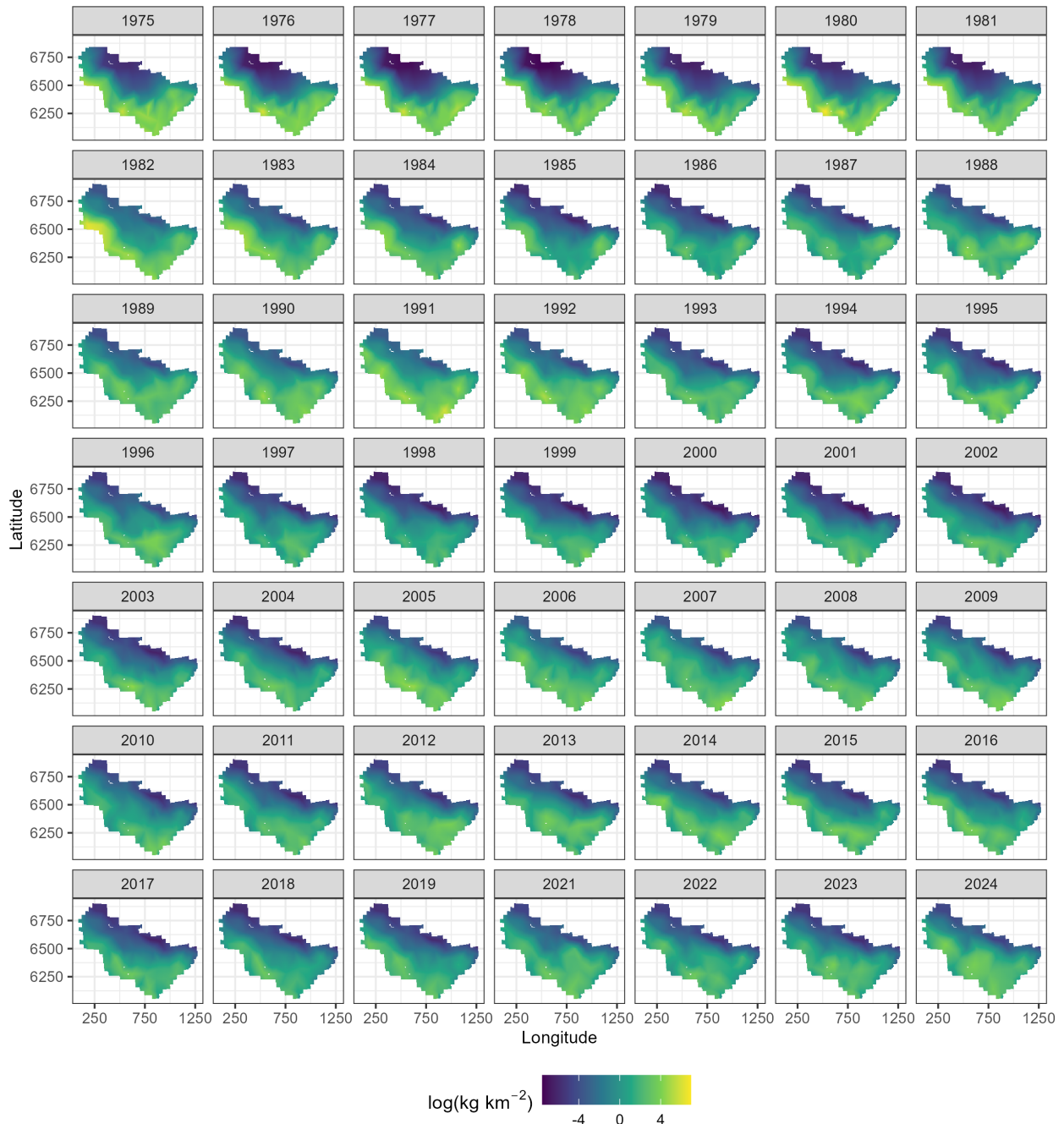


Figure 18: Spatial predictions of mature female biomass across the Eastern Bering Sea using NMFS summer bottom trawl survey data before 1982 and 1982 onward with a 50-knot mesh and a delta-gamma model family. Predictions from both of these periods/models are combined in this figure.

EBS Tanner estimated abundance

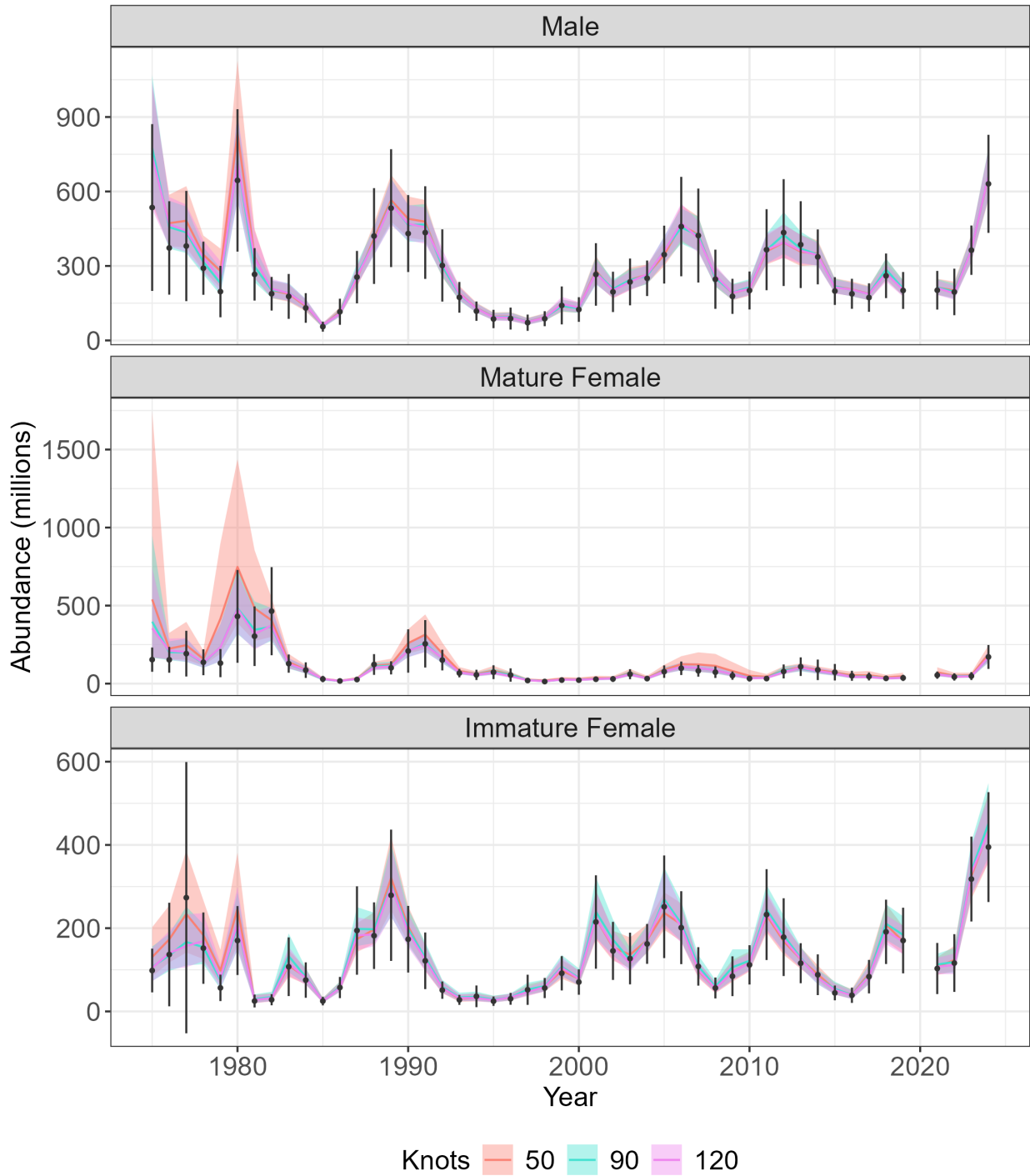


Figure 19: Estimated abundance (millions) for Tanner crab across the Eastern Bering Sea. Colored lines represent abundance ($\pm 95\%$ CI) estimated by sdmTMB, with orange, blue, and pink denoting models fit with a 50-, 90-, and 120-knot mesh, respectively. Black points represent abundance ($\pm 95\%$ CI) estimated by the NMFS summer bottom trawl survey.

EBS Tanner estimated biomass

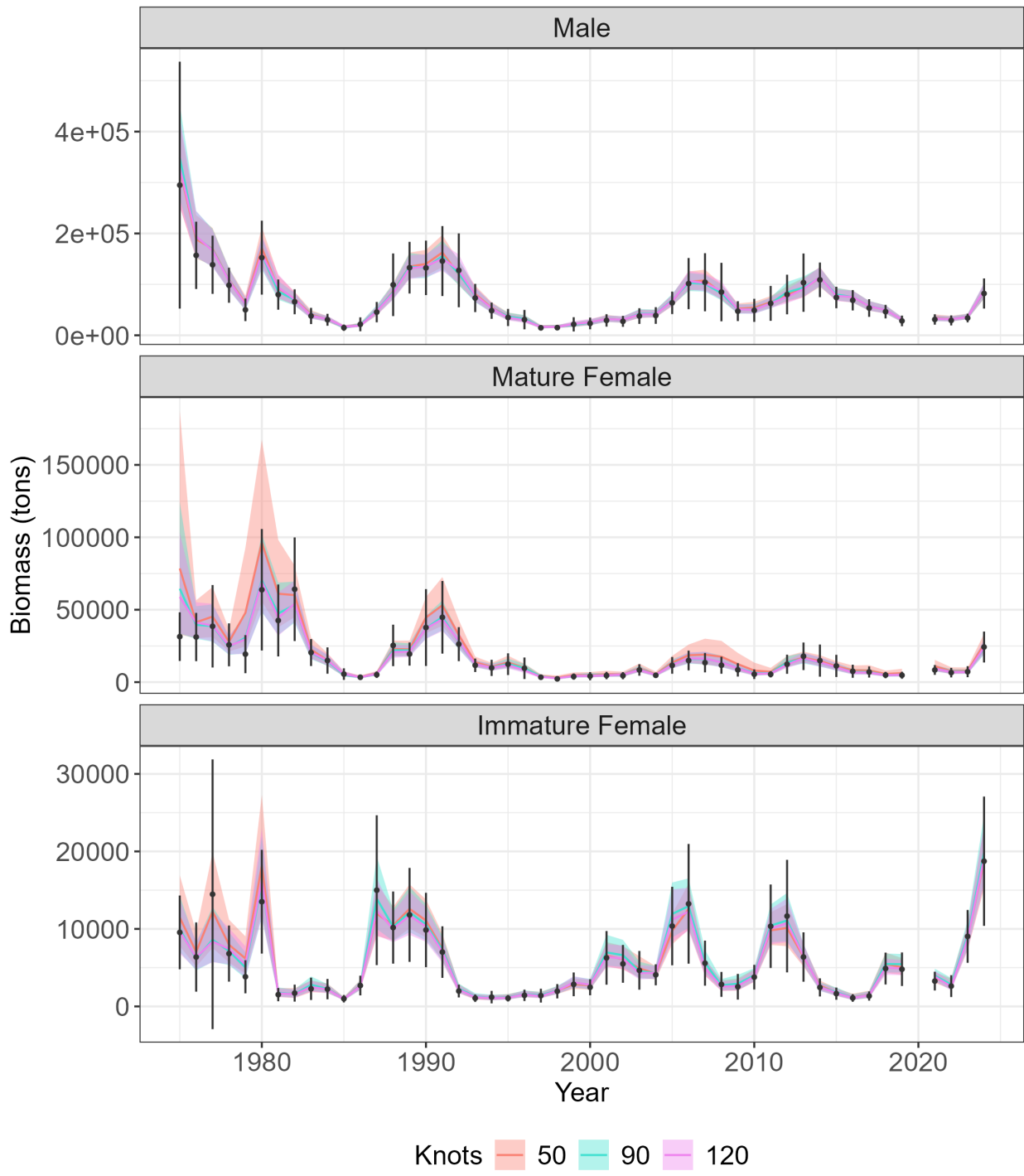


Figure 20: Estimated biomass (tons) for Eastern Bering Sea Tanner crab across the Eastern Bering Sea. Colored lines represent abundance ($\pm 95\%$ CI) estimated by sdmTMB, with orange, blue, and pink denoting models fit with a 50-, 90-, and 120-knot mesh, respectively. Black points represent biomass ($\pm 95\%$ CI) estimated by the NMFS summer bottom trawl survey.

Appendix

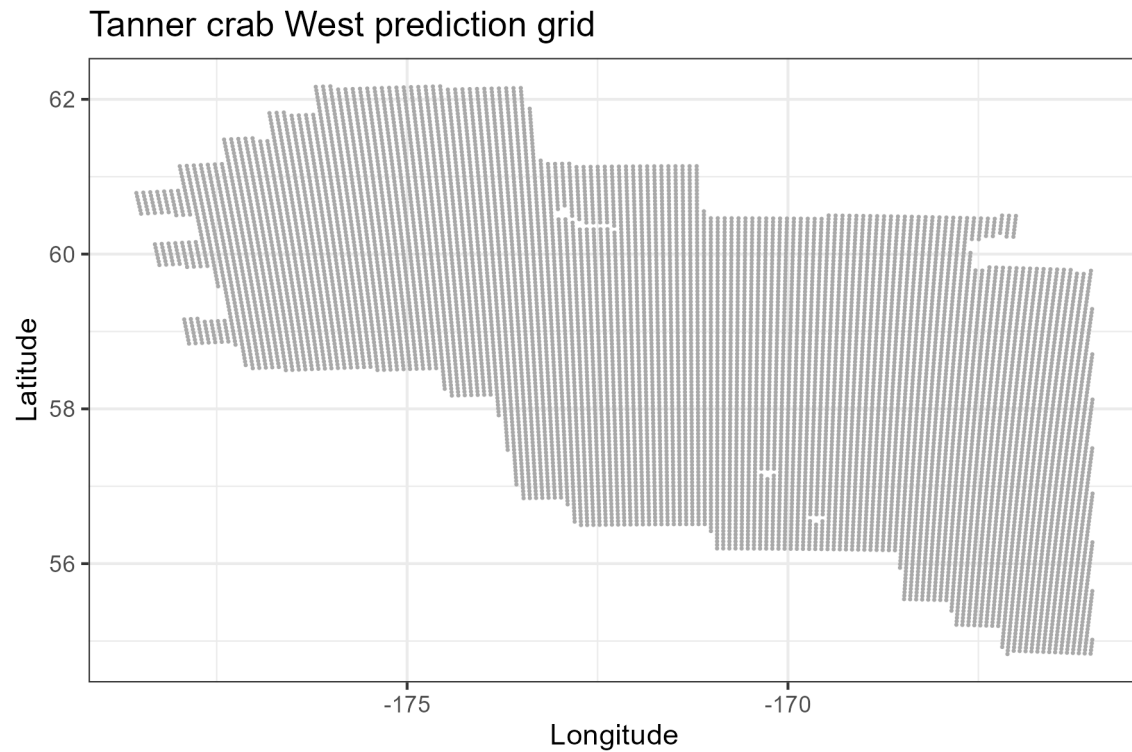


Figure 21: Prediction grid used to predict spatial abundance and biomass for Tanner crab west of 166° . Spatial resolution is 5km^2 and does not include land.

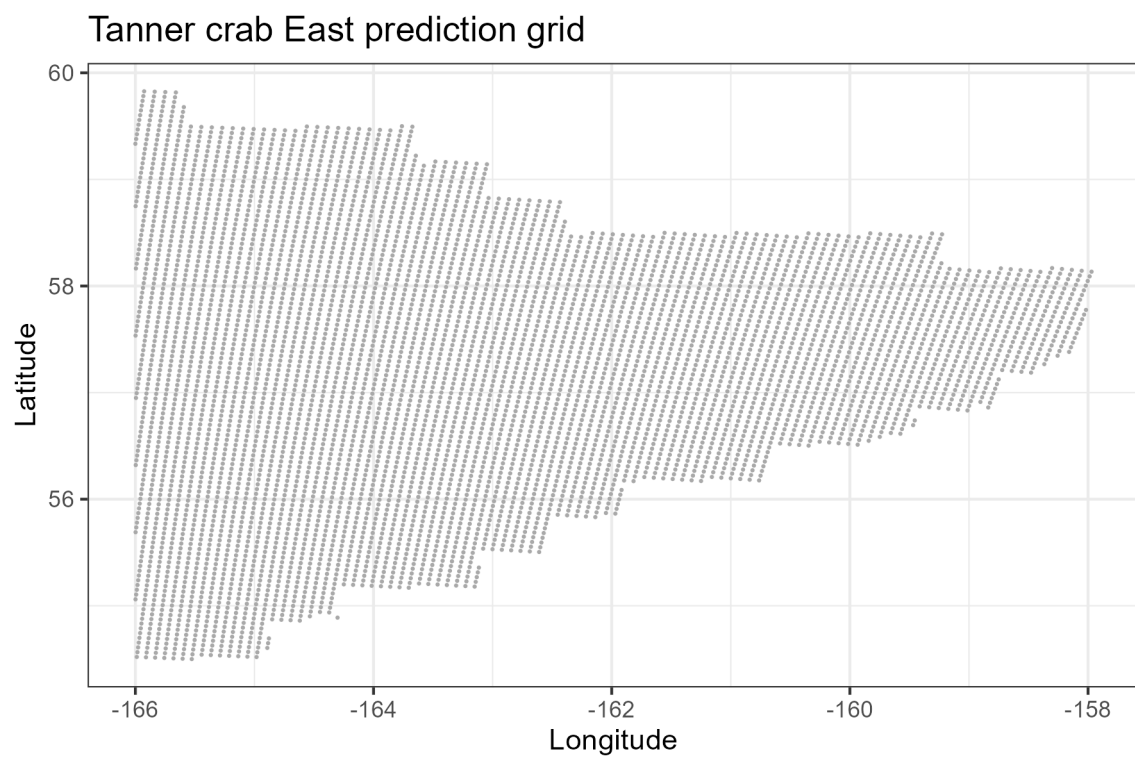


Figure 22: Prediction grid used to predict spatial abundance and biomass for Tanner crab east of 166° . Spatial resolution is 5km^2 and does not include land.

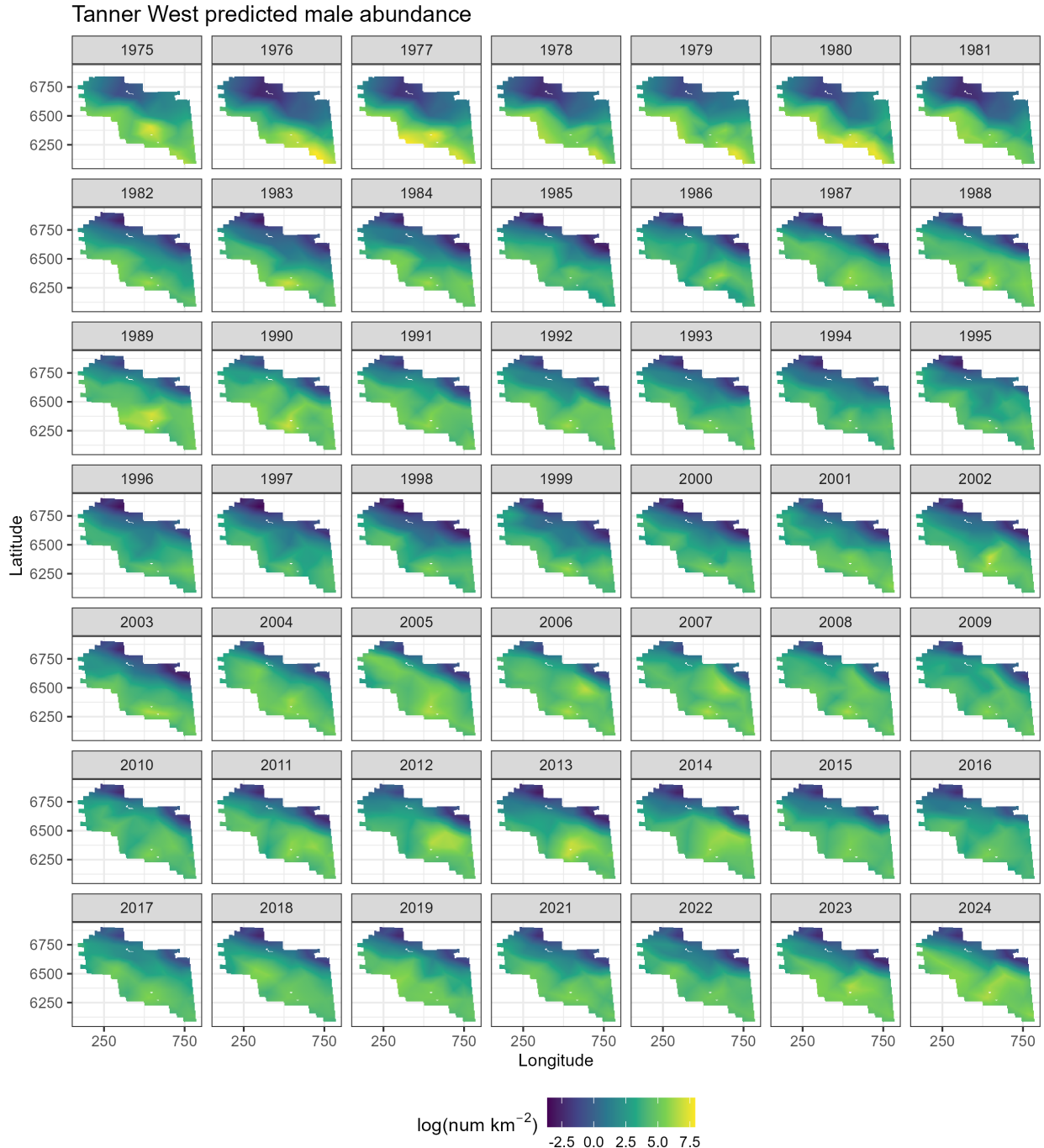


Figure 23: Spatial predictions of male abundance west of 166° using NMFS summer bottom trawl survey data before 1982 and 1982 onward with a 50-knot mesh and a delta-gamma model family. Predictions from both of these periods/models are combined in this figure.

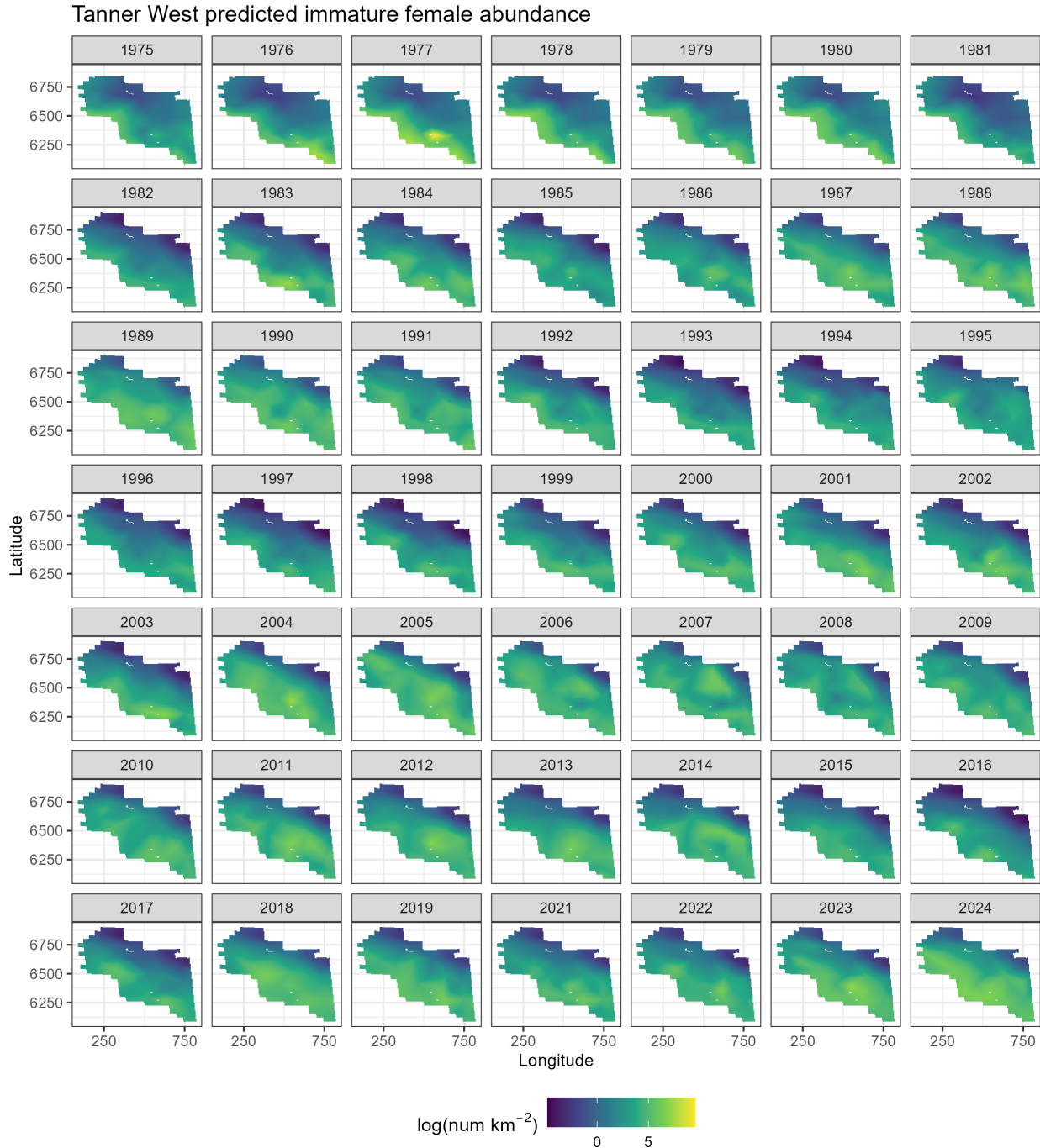


Figure 24: Spatial predictions of immature female abundance west of 166° using NMFS summer bottom trawl survey data before 1982 and 1982 onward with a 50-knot mesh and a delta-gamma model family. Predictions from both of these periods/models are combined in this figure.

Tanner West predicted mature female abundance

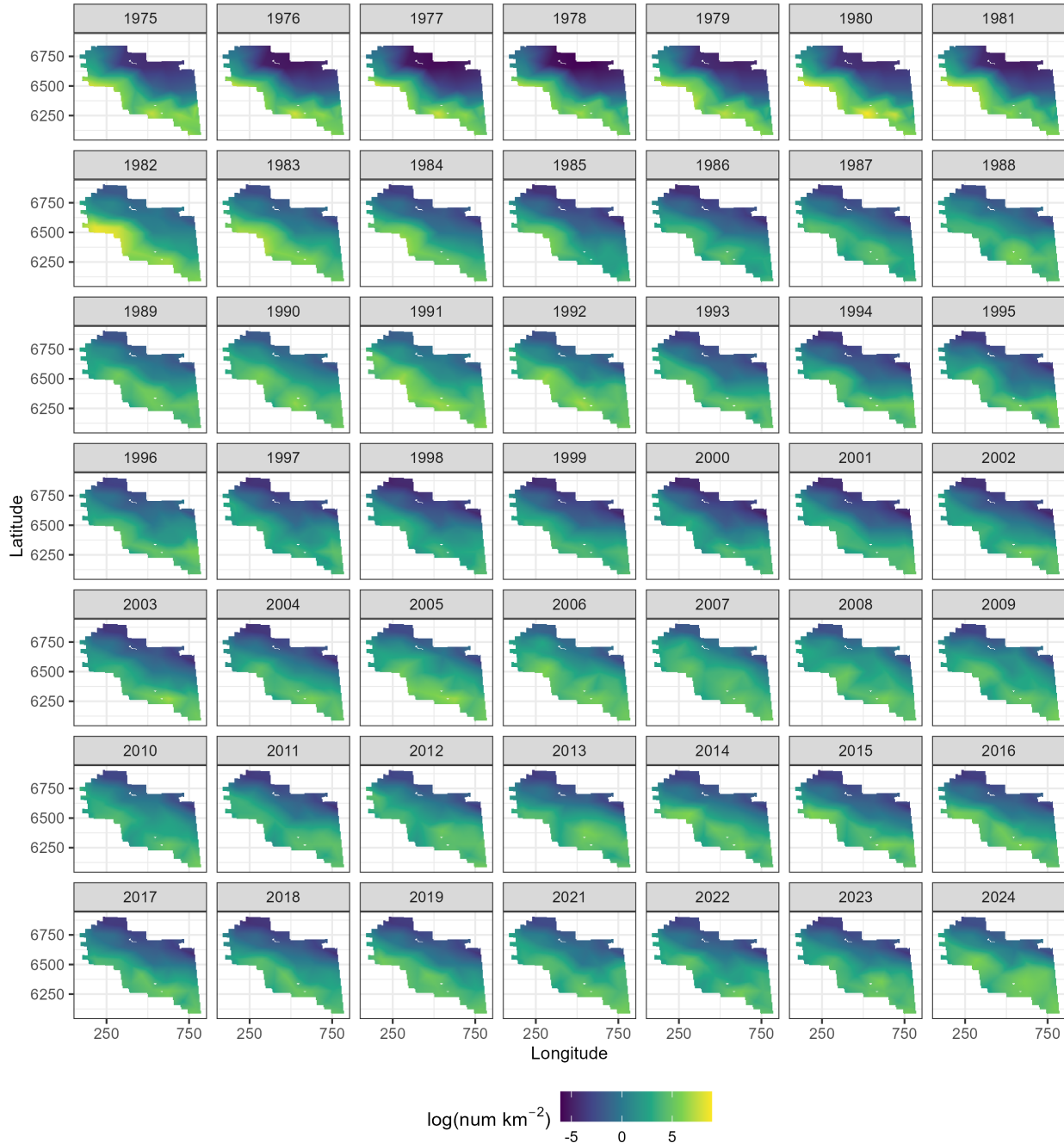


Figure 25: Spatial predictions of mature female abundance west of 166° using NMFS summer bottom trawl survey data before 1982 and 1982 onward with a 50-knot mesh and a delta-gamma model family. Predictions from both of these periods/models are combined in this figure.

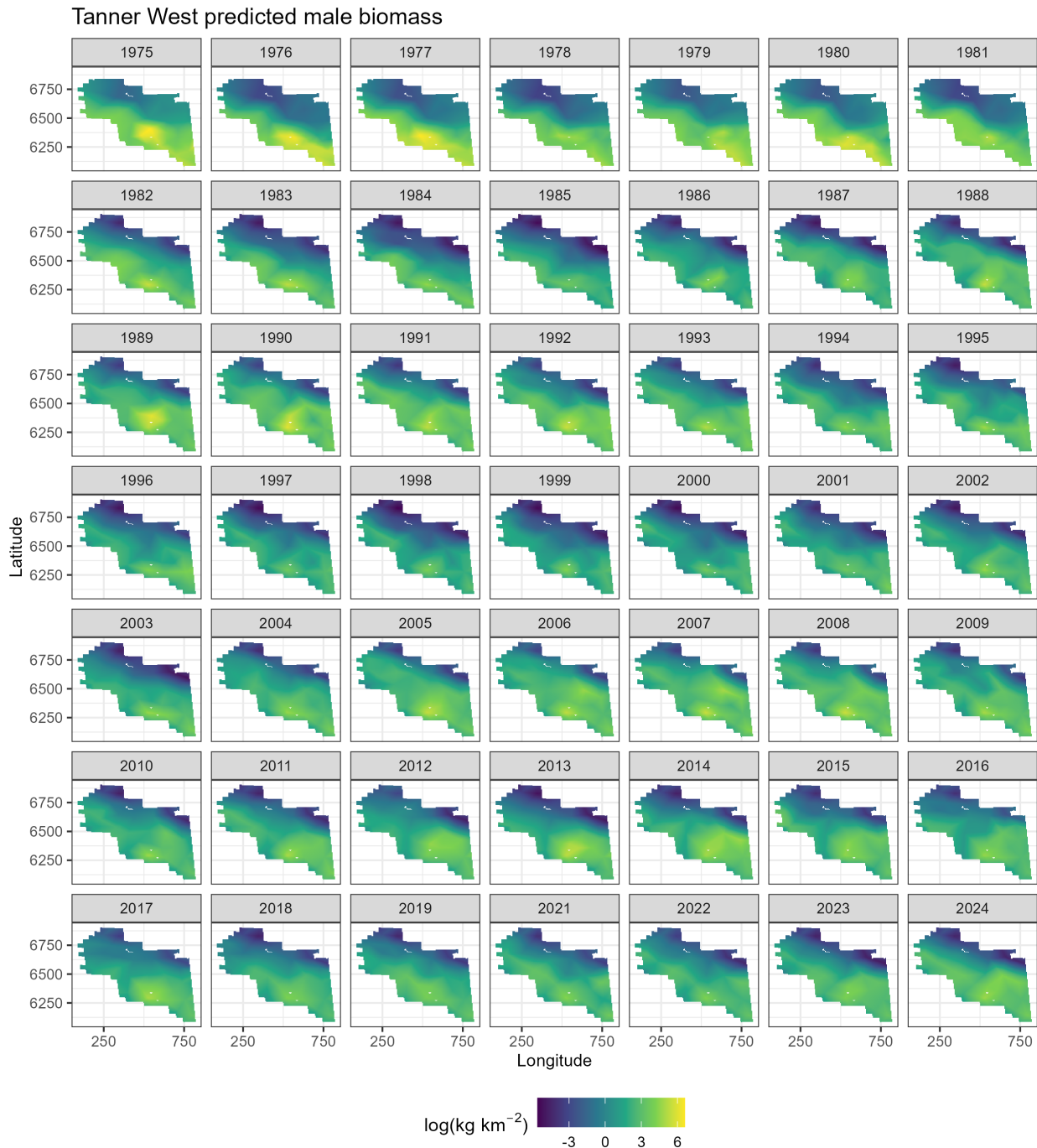


Figure 26: Spatial predictions of male biomass west of 166° using NMFS summer bottom trawl survey data before 1982 and 1982 onward with a 50-knot mesh and a delta-gamma model family. Predictions from both of these periods/models are combined in this figure.

Tanner West predicted immature female biomass

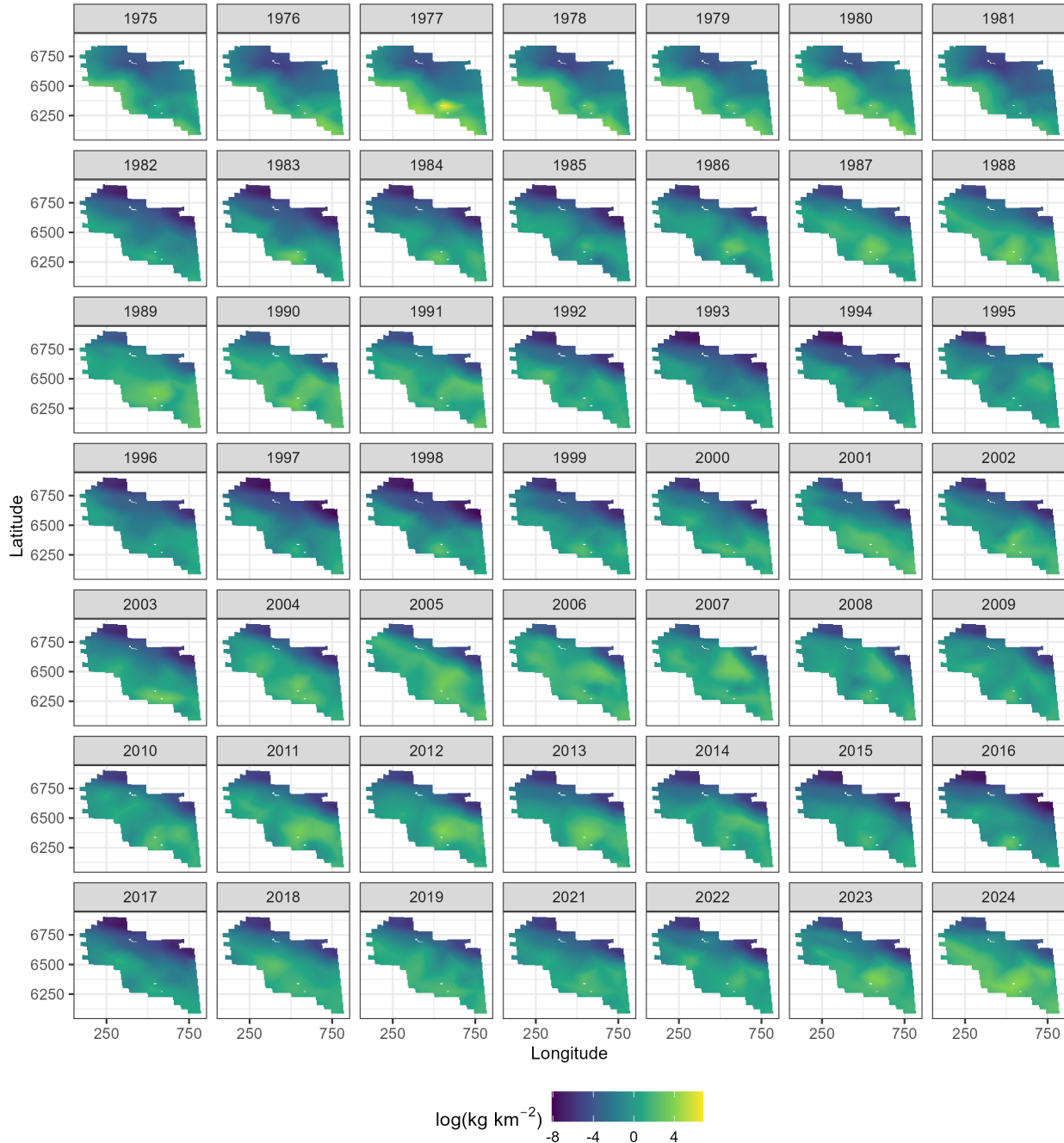


Figure 27: Spatial predictions of immature female biomass west of 166° using NMFS summer bottom trawl survey data before 1982 and 1982 onward with a 50-knot mesh and a delta-gamma model family. Predictions from both of these periods/models are combined in this figure.

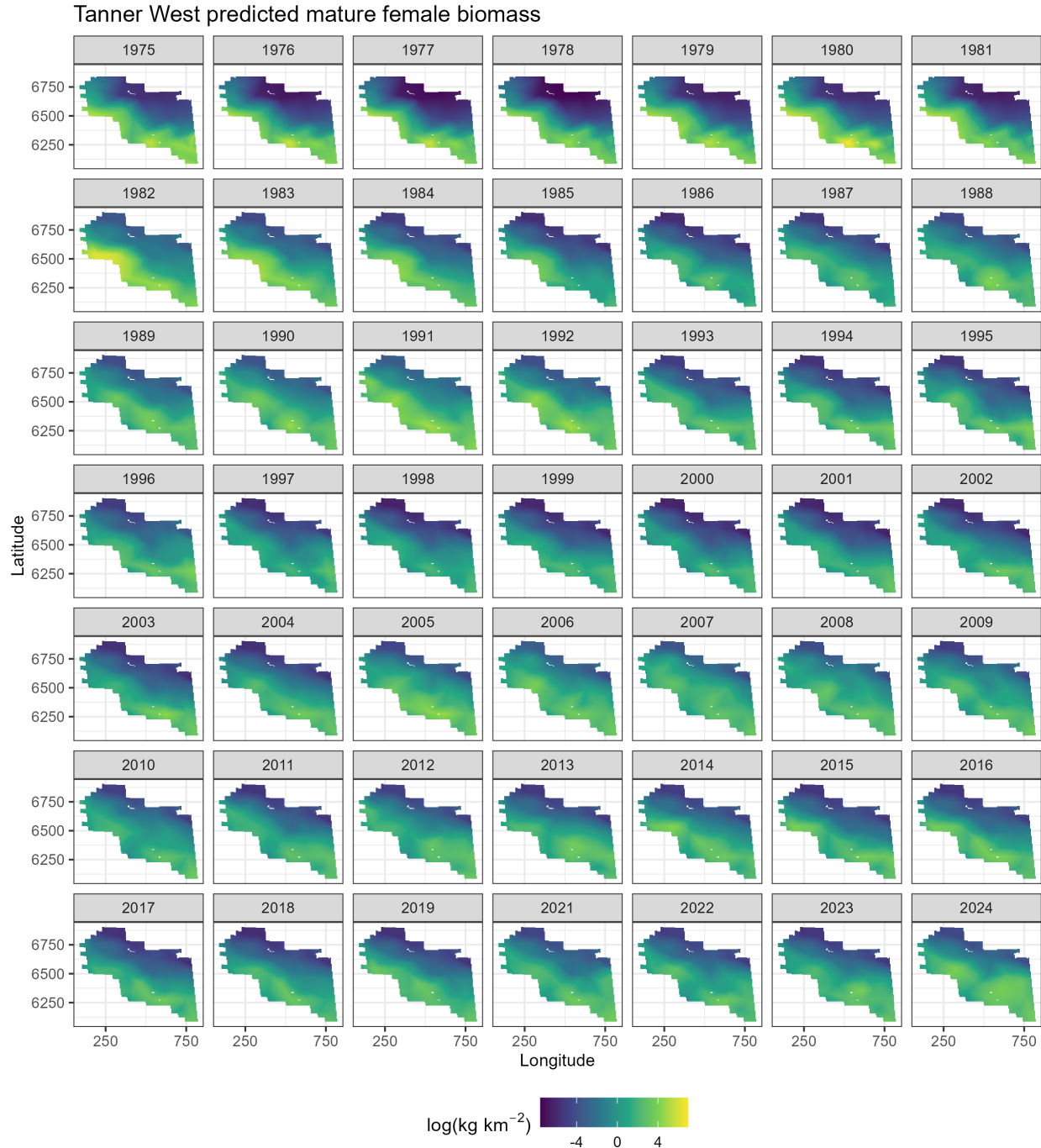


Figure 28: Spatial predictions of mature female biomass west of 166° using NMFS summer bottom trawl survey data before 1982 and 1982 onward with a 50-knot mesh and a delta-gamma model family. Predictions from both of these periods/models are combined in this figure.

Tanner East predicted male abundance

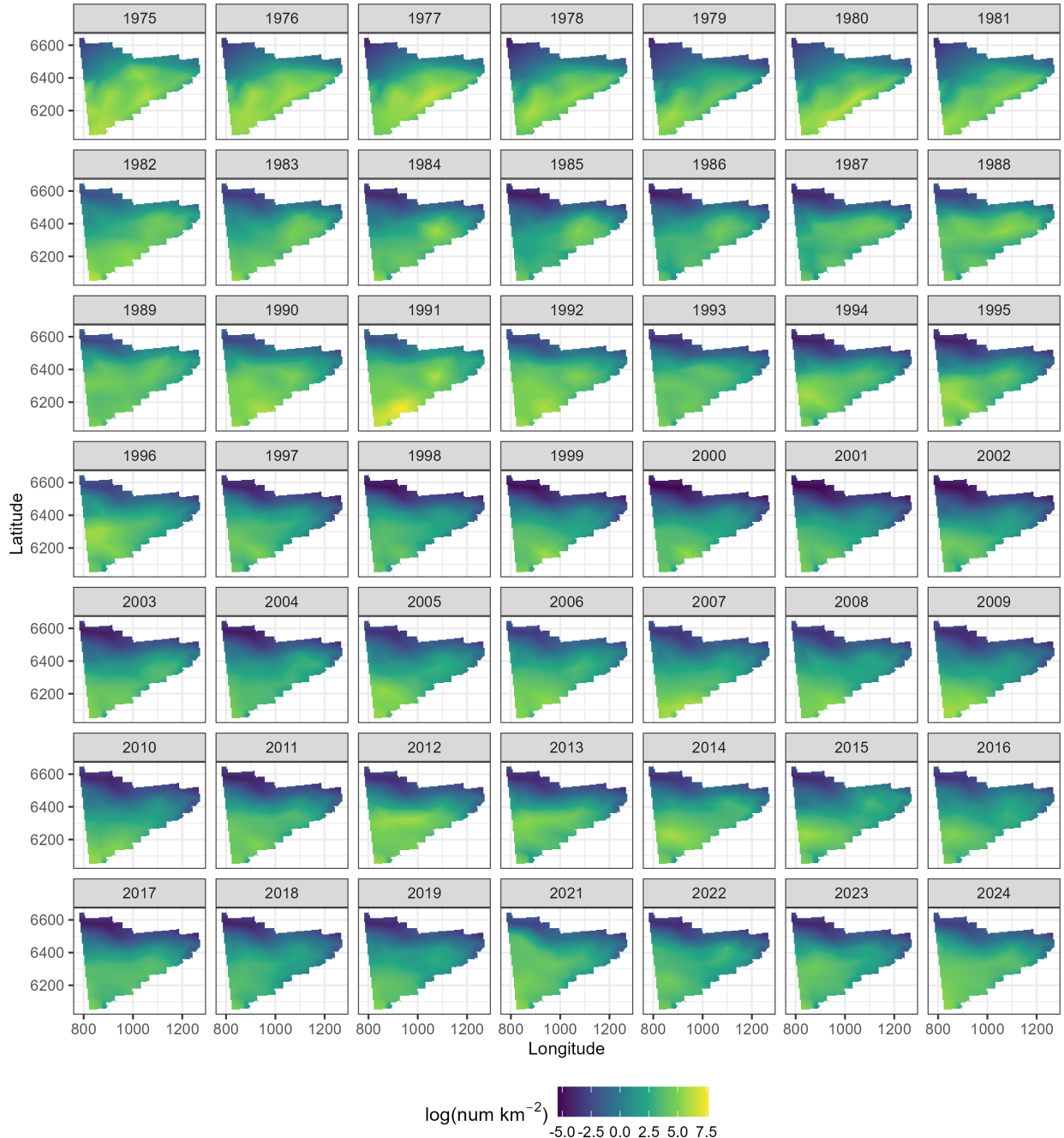


Figure 29: Spatial predictions of male abundance east of 166° using NMFS summer bottom trawl survey data before 1982 and 1982 onward with a 50-knot mesh and a delta-gamma model family. Predictions from both of these periods/models are combined in this figure.

Tanner East predicted immature female abundance

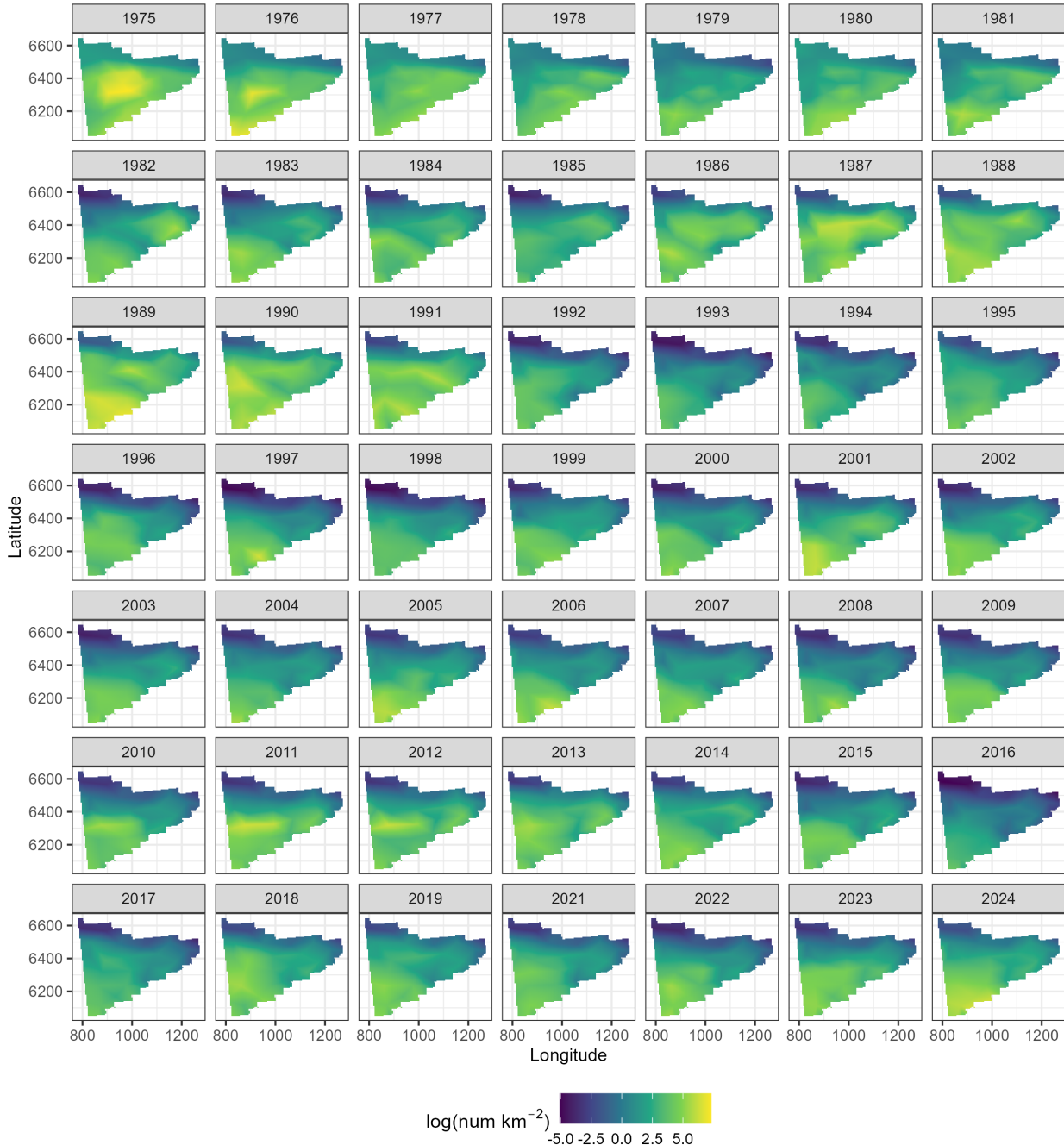


Figure 30: Spatial predictions of immature female abundance east of 166° using NMFS summer bottom trawl survey data before 1982 and 1982 onward with a 50-knot mesh and a delta-gamma model family. Predictions from both of these periods/models are combined in this figure.

Tanner East predicted mature female abundance

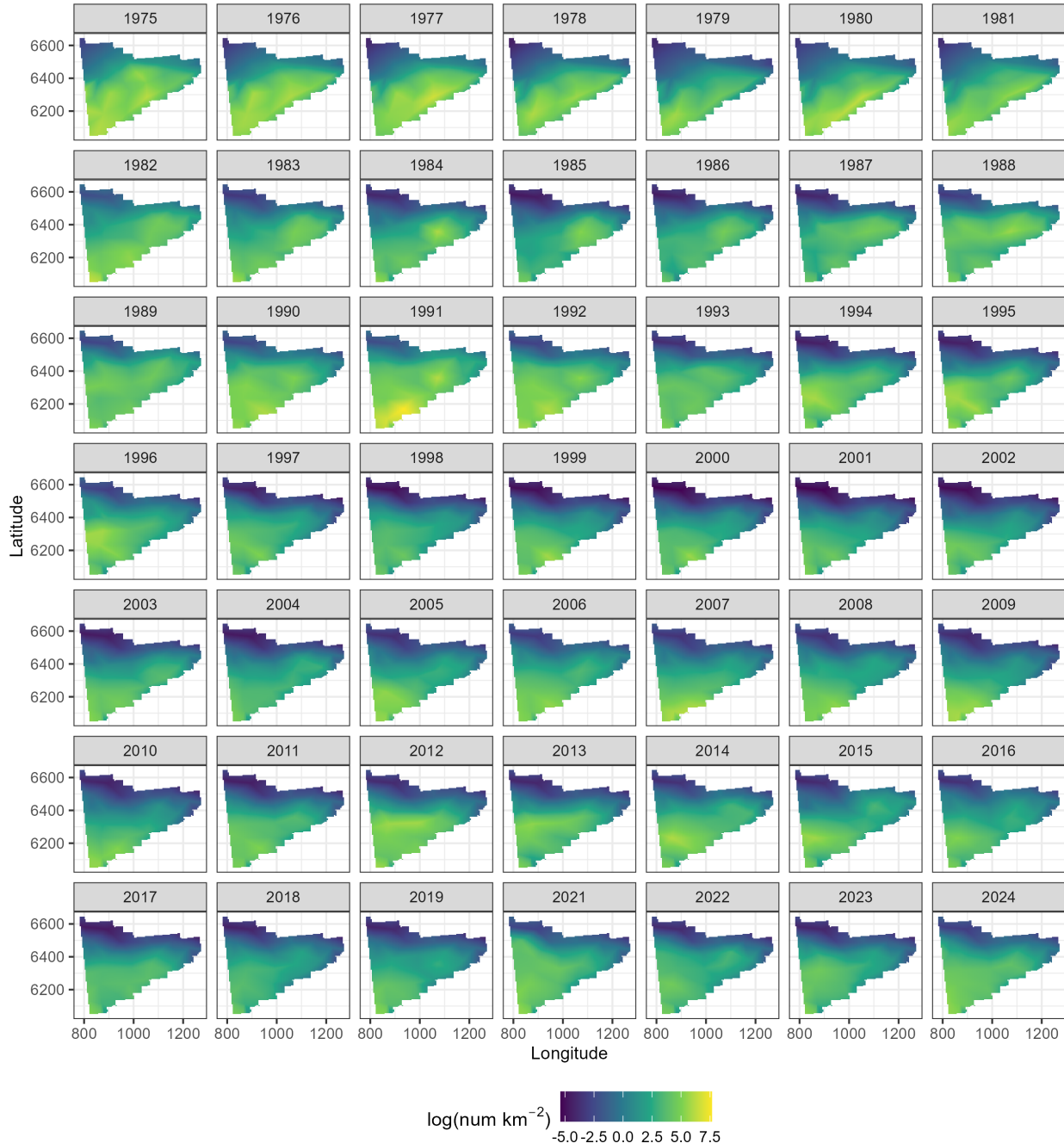


Figure 31: Spatial predictions of mature female abundance east of 166° using NMFS summer bottom trawl survey data before 1982 and 1982 onward with a 50-knot mesh and a delta-gamma model family. Predictions from both of these periods/models are combined in this figure.

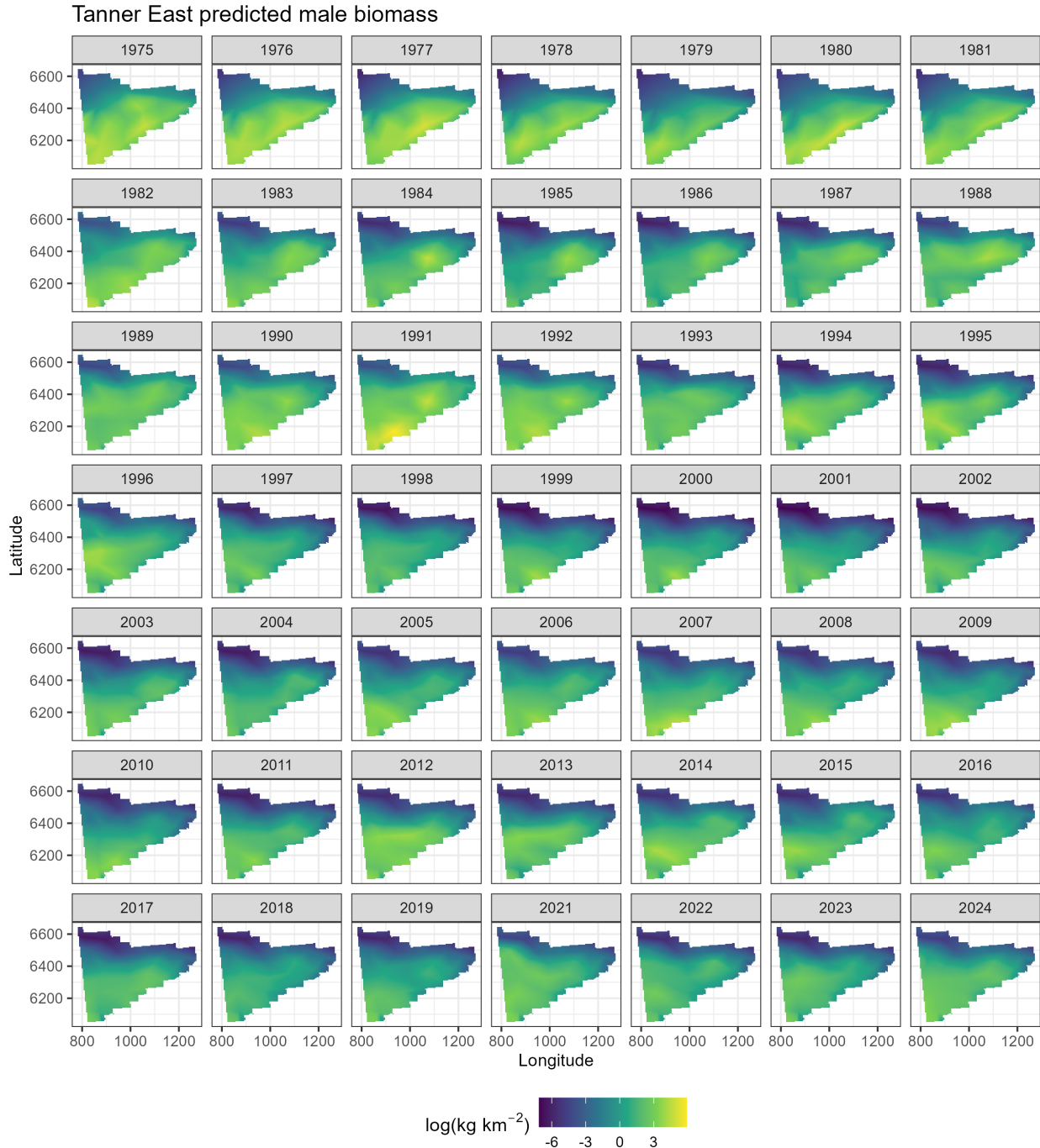


Figure 32: Spatial predictions of male biomass east of 166° using NMFS summer bottom trawl survey data before 1982 and 1982 onward with a 50-knot mesh and a delta-gamma model family. Predictions from both of these periods/models are combined in this figure.

Tanner East predicted immature female biomass

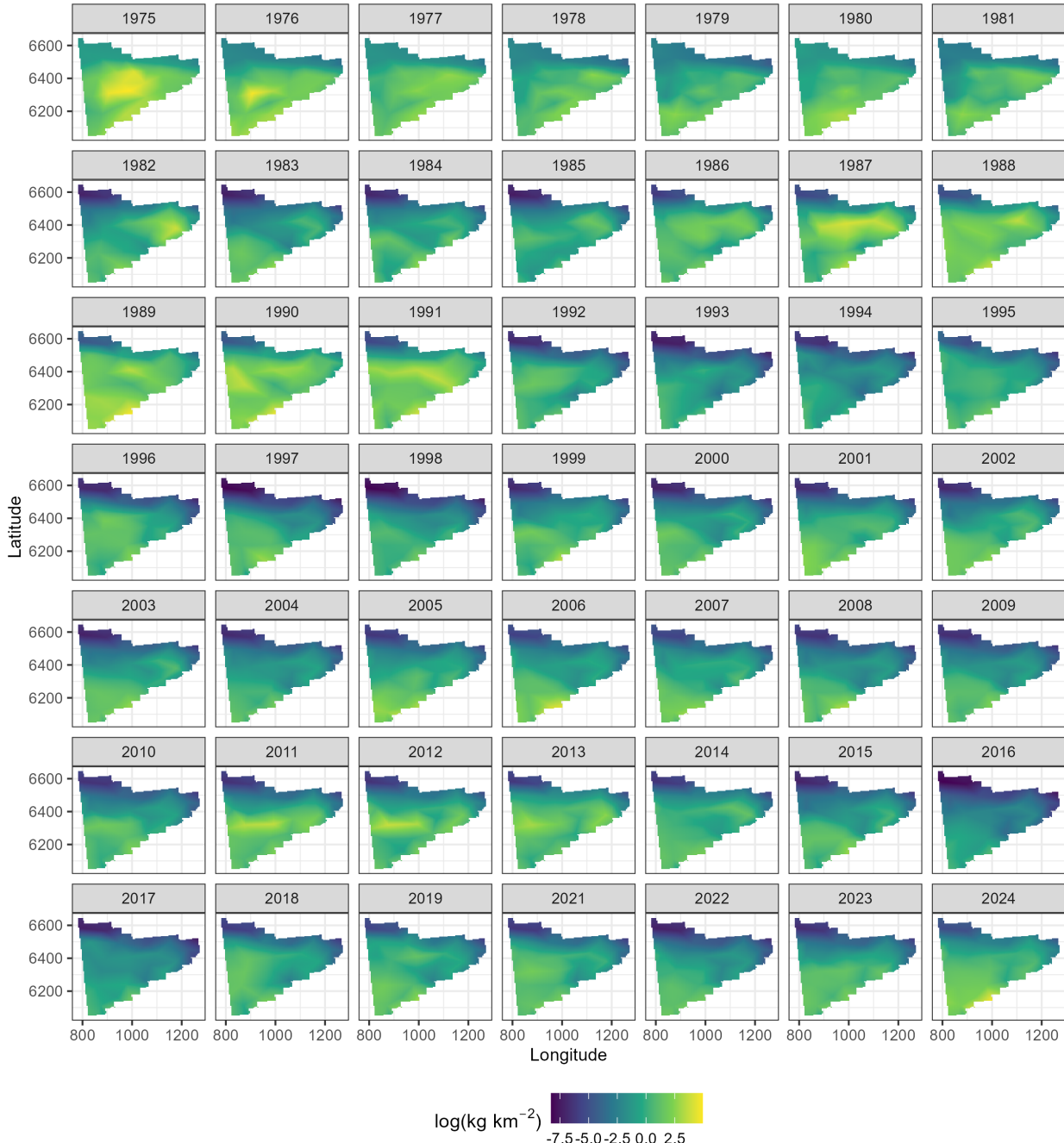


Figure 33: Spatial predictions of immature female biomass east of 166° using NMFS summer bottom trawl survey data before 1982 and 1982 onward with a 50-knot mesh and a delta-gamma model family. Predictions from both of these periods/models are combined in this figure.

Tanner East predicted mature female biomass

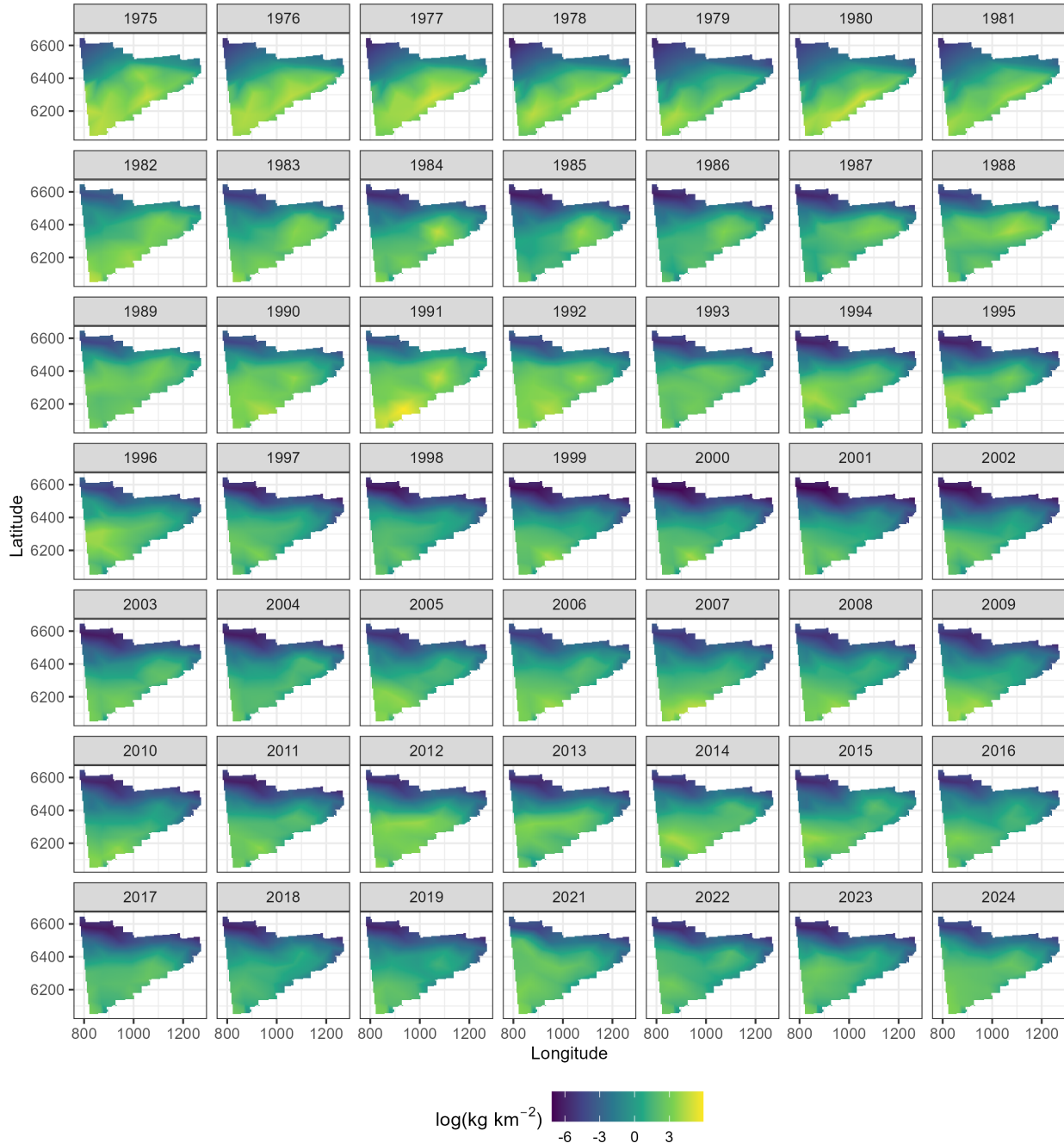


Figure 34: Spatial predictions of mature female biomass east of 166° using NMFS summer bottom trawl survey data before 1982 and 1982 onward with a 50-knot mesh and a delta-gamma model family. Predictions from both of these periods/models are combined in this figure.

Tanner West estimated abundance

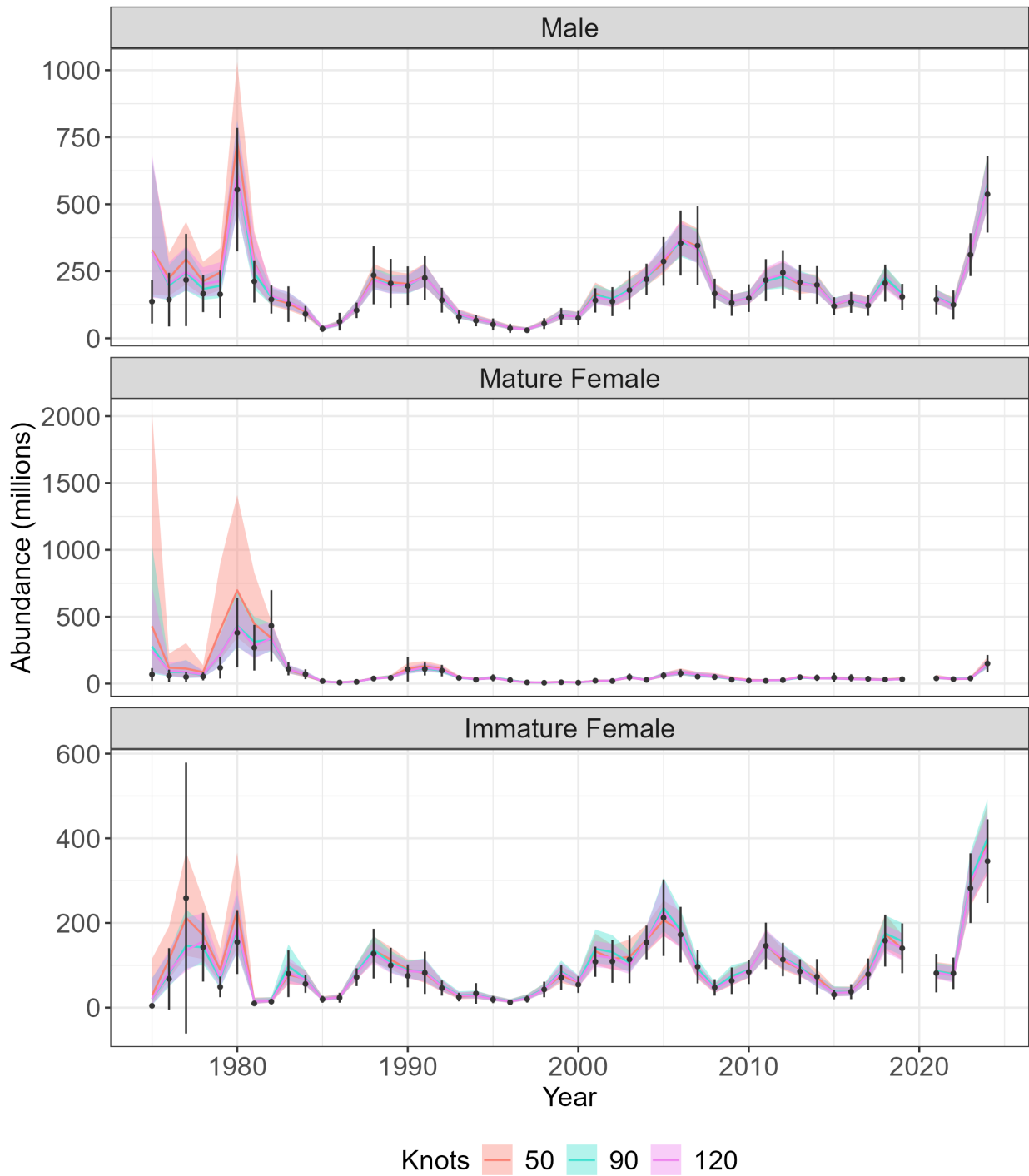


Figure 35: Estimated abundance (millions) for Tanner crab west of 166° . Colored lines represent abundance ($\pm 95\%$ CI) estimated by sdmTMB, with orange, blue, and pink denoting models fit with a 50-, 90-, and 120-knot mesh, respectively. Black points represent abundance ($\pm 95\%$ CI) estimated by the NMFS summer bottom trawl survey.

Tanner West estimated biomass

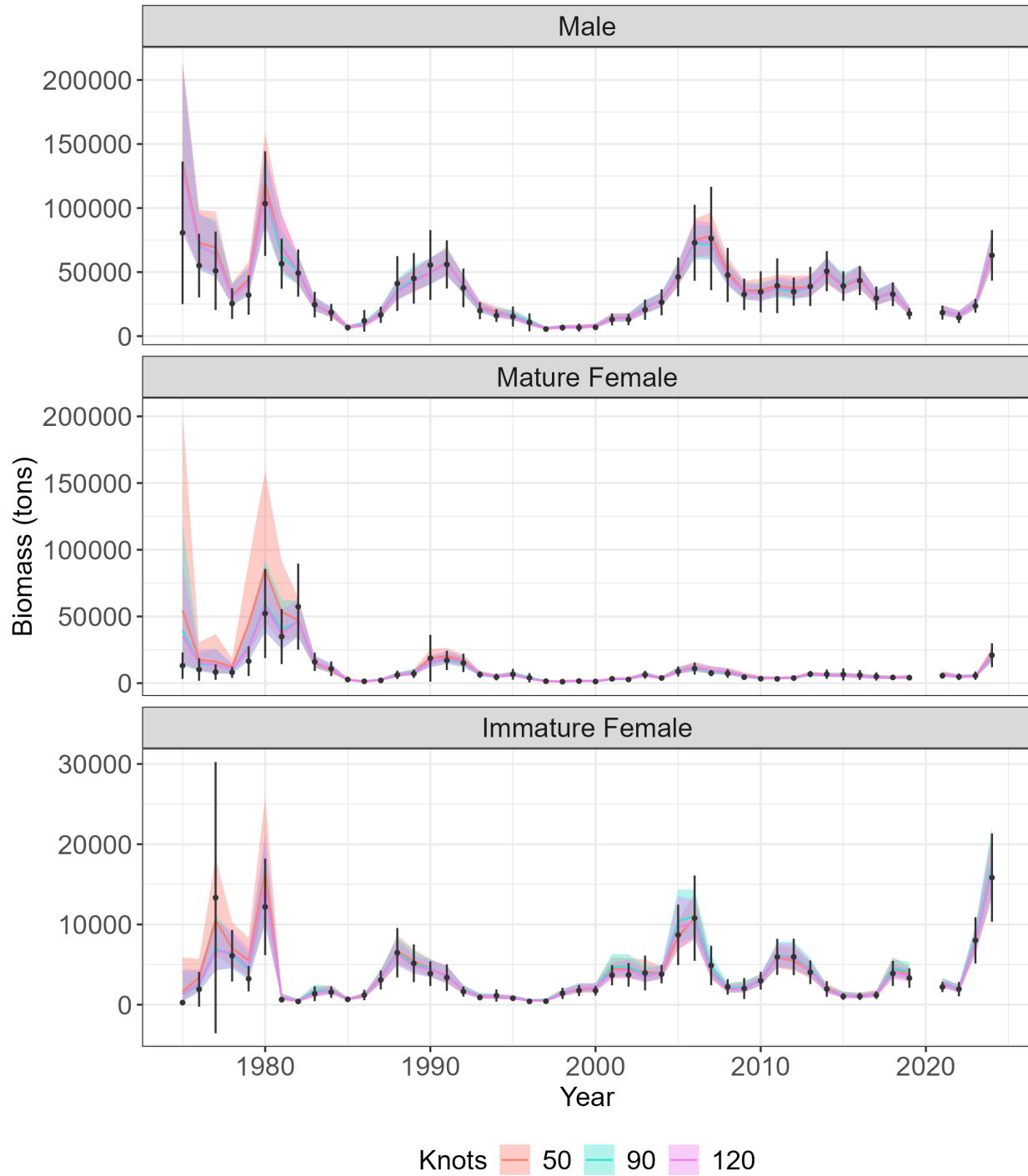


Figure 36: Estimated biomass (tons) for Eastern Bering Sea Tanner crab west of 166° . Colored lines represent abundance ($\pm 95\%$ CI) estimated by sdmTMB, with orange, blue, and pink denoting models fit with a 50-, 90-, and 120-knot mesh, respectively. Black points represent biomass ($\pm 95\%$ CI) estimated by the NMFS summer bottom trawl survey.

Tanner East estimated abundance

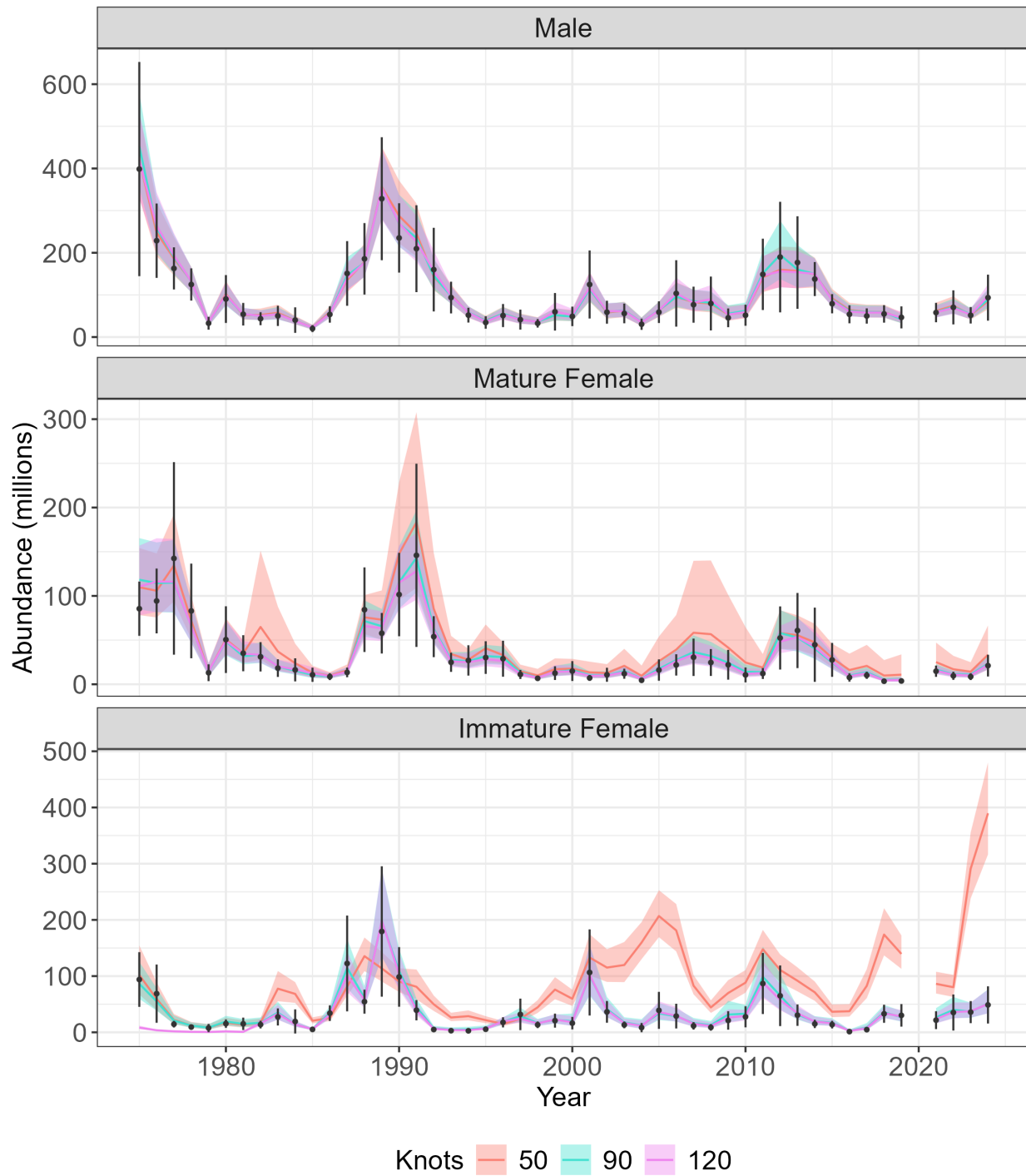


Figure 37: Estimated abundance (millions) for Tanner crab east of 166° . Colored lines represent abundance ($\pm 95\%$ CI) estimated by sdmTMB, with orange, blue, and pink denoting models fit with a 50-, 90-, and 120-knot mesh, respectively. Black points represent abundance ($\pm 95\%$ CI) estimated by the NMFS summer bottom trawl survey.

Tanner East estimated biomass

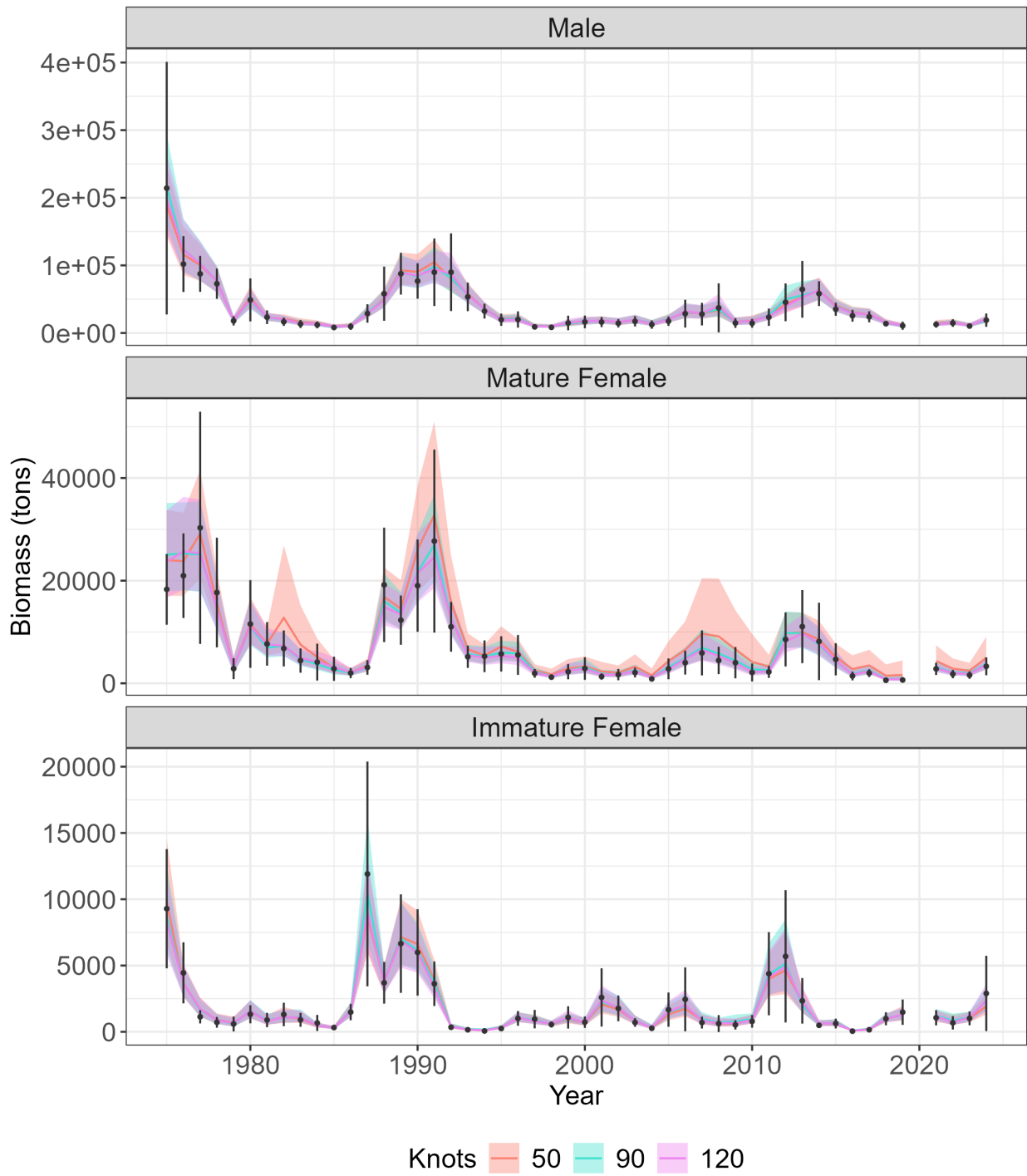


Figure 38: Estimated biomass (tons) for Eastern Bering Sea Tanner crab east of 166° . Colored lines represent abundance ($\pm 95\%$ CI) estimated by sdmTMB, with orange, blue, and pink denoting models fit with a 50-, 90-, and 120-knot mesh, respectively. Black points represent biomass ($\pm 95\%$ CI) estimated by the NMFS summer bottom trawl survey.